Journal of Chromatography A 1722 (2024) 464862

Contents lists available at ScienceDirect

Journal of Chromatography A

journal homepage: www.elsevier.com/locate/chroma

Size exclusion chromatography of biopharmaceutical products: From current practices for proteins to emerging trends for viral vectors, nucleic acids and lipid nanoparticles

Valentina D'Atri [a,b], Mateusz Imiołek [c], Colette Quinn [d], Abraham Finny [e], Matthew Lauber [e], Szabolcs Fekete [c], Davy Guillarme [a,b,*]

[a] Institute of Pharmaceutical Sciences of Western Switzerland, University of Geneva, CMU - Rue Michel Servet 1,4, 1211 Geneva, Switzerland
[b] School of Pharmaceutical Sciences, University of Geneva, CMU - Rue Michel Servet 1,4, 1211 Geneva, Switzerland
[c] Waters Corporation, Geneva, Switzerland
[d] Waters Corporation, Milford, MA, USA
[e] Waters Corporation, Wyatt Technology, Santa Barbara, CA, USA

ARTICLE INFO

Keywords:
Size exclusion chromatography
Gene therapy
Messenger RNA
Monoclonal antibodies
Bioinert columns
New modalities

ABSTRACT

The 21st century has been particularly productive for the biopharmaceutical industry, with the introduction of several classes of innovative therapeutics, such as monoclonal antibodies and related compounds, gene therapy products, and RNA-based modalities. All these new molecules are susceptible to aggregation and fragmentation, which necessitates a size variant analysis for their comprehensive characterization. Size exclusion chromatography (SEC) is one of the reference techniques that can be applied. The analytical techniques for mAbs are now well established and some of them are now emerging for the newer modalities. In this context, the objective of this review article is: *i)* to provide a short historical background on SEC, *ii)* to suggest some clear guidelines on the selection of packing material and mobile phase for successful method development in modern SEC; and *iii)* to highlight recent advances in SEC, such as the use of narrow-bore and micro-bore columns, ultra-wide pore columns, and low-adsorption column hardware. Some important innovations, such as recycling SEC, the coupling of SEC with mass spectrometry, and the use of alternative detectors such as charge detection mass spectrometry and mass photometry are also described. In addition, this review discusses the use of SEC in multidimensional setups and shows some of the most recent advances at the preparative scale. In the third part of the article, the possibility of SEC for the characterization of new modalities is also reviewed. The final objective of this review is to provide a clear summary of opportunities and limitations of SEC for the analysis of different biopharmaceutical products.

1. Introduction

In recent years, the pharmaceutical industry has been evolving towards the development of several innovative biotherapeutics that are significantly larger than the classical small molecules. These large biologics, often produced by living organisms or new, multistep cell-free processes, can be used to address previously intractable diseases [1,2]. The development of biopharmaceutical products started at the beginning of the 21st century with the development of monoclonal antibodies (mAbs) and mAb-related compounds such as fusion proteins, bispecific antibodies, and antibody-drug conjugates (ADCs) [3,4]. These molecules have been spectacularly successful in the clinic, and it could be said that this form of biotechnology is reaching a state of comparative maturity. In 2020 and 2021, 20 mAb-based products were approved each year in the world [5]. The mAb market reached 162 billion USD in 2021 and is expected to expand to 390 billion USD by 2030 with nearly 800 mAb therapeutics in development in oncology, representing more than 60% of the clinical pipeline [5,6]. The anti-PD-1 immune checkpoint inhibitor pembrolizumab has been pivotal to unlocking the potential of cancer treatments [7,8]. In addition to mAb products, there is also a wide range of other new modalities that are reshaping the pharmaceutical market. One of the main modalities driving this market evolution can be classified as gene therapies, which aim to modify or manipulate gene expression of living cells for therapeutic purposes [9].

* Corresponding author.
E-mail address: davy.guillarme@unige.ch (D. Guillarme).

https://doi.org/10.1016/j.chroma.2024.464862
Received 1 March 2024; Received in revised form 29 March 2024; Accepted 31 March 2024
Available online 1 April 2024

Gene therapy products include DNA plasmids, viral vectors, and human gene editing technologies, for example drug products that are created with CRISPR-Cas technology [10–12]. The current US pipeline is expected to yield 66 approvals of such therapies by 2032 [13]. In addition, RNA-based molecules such as antisense RNA, small interfering RNA, micro-RNA, RNA aptamers and messenger RNA (mRNA) have attracted much attention, given their ability to regulate protein expression [14–17]. These molecules are usually delivered by carriers, such as viral vectors or lipid nanoparticles [18,19]. As recently highlighted, [20] therapies with small molecules and mAbs are inherently limited, as they can target only 0.05% of the human genome since many disease targets lack active sites to bind small molecules. On the other hand, RNA can selectively target proteins, transcripts, and genes, which expands the range of druggable targets. Currently, there are numerous RNA-based drugs that have already been approved and many more are in phase 3 trials. These RNA drugs are being used to treat both rare and common diseases.

Given the unique physicochemical properties of the emerging drugs discussed above, it is easy to understand that they can undergo various changes during their preparation, formulation, and storage. These modifications may compromise therapeutic efficacy, increase toxicity or increase the side effects for the patients. Therefore, it is imperative to comprehensively characterize these molecules, using a variety of analytical techniques to evaluate their structural, functional, and physicochemical properties. Size-based separation techniques are particularly important as fragments and aggregates are often present in these large molecules. These product-related impurities are frequently assigned as being critical quality attributes (CQAs) [21,22].

Several sized-based separation techniques are currently available and can be considered. First, asymmetric flow field flow fractionation (A4F) separates analytes based on their size and shape, as they flow through a thin channel. It uses a liquid that moves through the channel at different speeds, allowing diffusion-based separation of large and small molecules. This technique is particularly attractive for the analysis of soluble proteins and nanoparticles [23,24,25]. Another possibility is the use of analytical ultracentrifugation (AUC). In this case, the sample is subjected to high-speed centrifugal forces that cause shape and size-based sedimentation of particles. Estimates on sedimentation rate can be then correlated with the molecular weight of the macromolecules in the sample [26,27]. A third option is capillary gel electrophoresis (CGE), which uses an electric field to separate charged molecules in a capillary filled with a gel. The smaller the molecule is, the faster it migrates through the gel, which is the principle providing a size-based separation. Thanks to the capillary format, it is possible to dramatically improve resolution and efficiency as compared to classical gel electrophoresis [28,29,30]. Size exclusion chromatography (SEC) is also a viable approach for achieving size-based separation. Finally, multi-angle light scattering (MALS) measures the scattered light at different angles as it interacts with particles in solution. The size and molecular weight of large molecules can then be determined by analyzing the scattered light patterns [31,32]. Importantly, MALS can be easily combined with SEC and A4F to provide detailed information on molecular characteristics.

In recent years, several reviews have been published on the application of SEC to the analysis of mAbs. The primary aim of this article is to extend this knowledge beyond mAbs. Furthermore, we would like to provide a clear strategy for method development in modern SEC using columns packed with sub-3 μm particles. The goal is also to highlight some of the most recent advances in SEC, including the use of narrow-bore and micro-bore SEC columns, ultra-wide pore SEC columns, and low-adsorption (often referred to as "bioinert") column hardware. Some innovations are also explored, such as recycling SEC, the coupling of SEC with mass spectrometry and alternative detectors (such as charge detection mass spectrometry and mass photometry), SEC incorporation into multidimensional LC setups, and important developments at the preparative scale.

2. Fundamental principles of SEC

SEC is one of the most widely used sized-based separation techniques, which separates species based on their hydrodynamic radius. The SEC principle of operation is quite simple, and is illustrated in Fig. 1. As the sample flows through the column, molecules could be either totally excluded from the pores of the stationary phase (if they are sufficiently large), they could fully penetrate into the pores (if they are small enough), or the molecules can be partially excluded from the pores (which is the common case when a column with an appropriate pore size is selected). Large molecules travel faster through the column with the mobile phase as they do not penetrate the pores. On the contrary, small molecules take longer to elute from the column, as they spend more time inside the pores.

The success of SEC can be explained by the fact that the technique can be applied to the characterization of various commercial and emerging biotherapeutics in time and cost-effective manner. It has several advantages including its excellent quantitative performance, ease of use, and favorable perception by regulatory authorities. SEC is an entropically controlled separation technique. It operates under mild chromatographic conditions, allowing the analysis of biological molecules with minimal impact on their conformation (native conditions) [33]. Consequently, SEC is considered to be a non-denaturing chromatographic mode [34].

The stationary phase in SEC is composed of spherical, porous particles, with precisely controlled pore sizes and pore size distributions, which allows the differentiation of molecules based on their molecular size, without physicochemical interactions [35]. To minimize the possible interactions between the molecule of interest and the SEC column, all components must be inert. Therefore, surface modifications, such as derivatization with hydrophilic silanes, diol functionalization and methyl- or hydroxy-terminated polyethylene oxide bonding are often considered. In conventional SEC, large columns (e.g., 300 × 8 mm) packed with 5 μm particles are commonly used at low flow rates and pressures. Under such conditions, analysis times typically range from 25 to 40 min. Since all peaks elute before the column hold-up time (t_M), it is generally necessary to perform SEC with a comparatively large volume column to allow sufficient time for the separation [36].

Once the appropriate SEC column has been selected, it is important to optimize the mobile phase composition. Physiological conditions at a pH between 6.2 and 7.5 are typically used. A phosphate buffer (50 - 200 mM) is a common buffering agent for this pH range [37]. In addition, it is common practice to add a significant amount of potassium or sodium salts (from 200 to 400 mM of KCl or NaCl) to the mobile phase. This helps limit unwanted secondary electrostatic interactions between the analytes and the packing material [38].

3. Steps towards modern SEC

3.1. Columns packed with sub-3 μm particles: the new reference material

A popular strategy to improve performance (speed and efficiency) in LC is to use columns packed with smaller and smaller particles. Reverse phase columns packed with sub-2 μm porous particles were commercially introduced in 2004, and SEC columns of the same type were first available in 2011 (i.e. a BEH™ 200 Å SEC Column packed with 1.7 μm particles). This column is considered to be the precursor of modern SEC, also known as ultra-high-performance SEC (UHP-SEC). The rationale behind the use of columns packed with smaller sized particles is to improve column efficiency by reducing both the eddy dispersion (*A* term in the common plate height equation) and the mass transfer resistance (*C* term). When comparing the performance of columns packed with sub-2 μm particles and columns packed with 3 or 5 μm particles, plate heights were 2 to 5 times lower with the 1.7 μm packing. This means that similar plate count can be obtained in standard SEC and modern SEC, but the latter offers a reduction in analysis times by a factor of 2 to 4

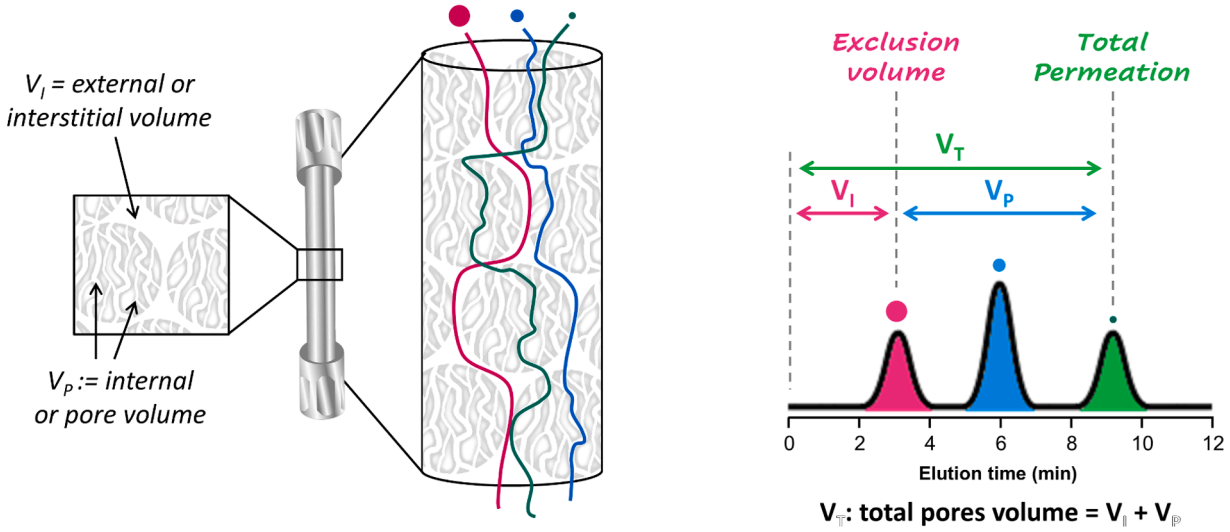

Fig. 1. SEC principle of operation. Schematic picture of a SEC column with an inserted enlargement and graphical description of the separation process. An hypothetical chromatogram is also provided and shows corresponding V_I, V_T and V_P values.

[39]. Based on these attractive features, many suppliers have recently introduced SEC columns packed with sub-3 μm particles. In a systematic comparison performed in our laboratory in 2017, with different model proteins, commercial therapeutic mAbs and ADCs samples, kinetic performance evaluation (plate height curves and kinetic plots) showed that SEC columns packed with 1.7 - 2.0 μm particles improved plate count by 1.5 - 2 times compared to 2.7 - 3.0 μm particles, in line with theoretical expectations [40]. In addition to kinetic performance, non-specific interactions between the analyzed proteins and the stationary phases were also investigated, and it was shown that hydrophobic interactions were more critical than electrostatic interactions, with strong differences between the four modern SEC columns that were compared, as shown in Fig. 2 for two mAbs and two ADCs samples.

These non-specific interactions are responsible for strong peak distortion and broadening as well as elution time shifts. Combining both kinetic performance and non-specific interactions, the four SEC columns packed with sub-3 μm particles showed comparable resolution when analyzing a diverse set of 10 different commercial mAb products. In fact, the resolution between monomers and dimers ranged from 1.6 to 2.4,

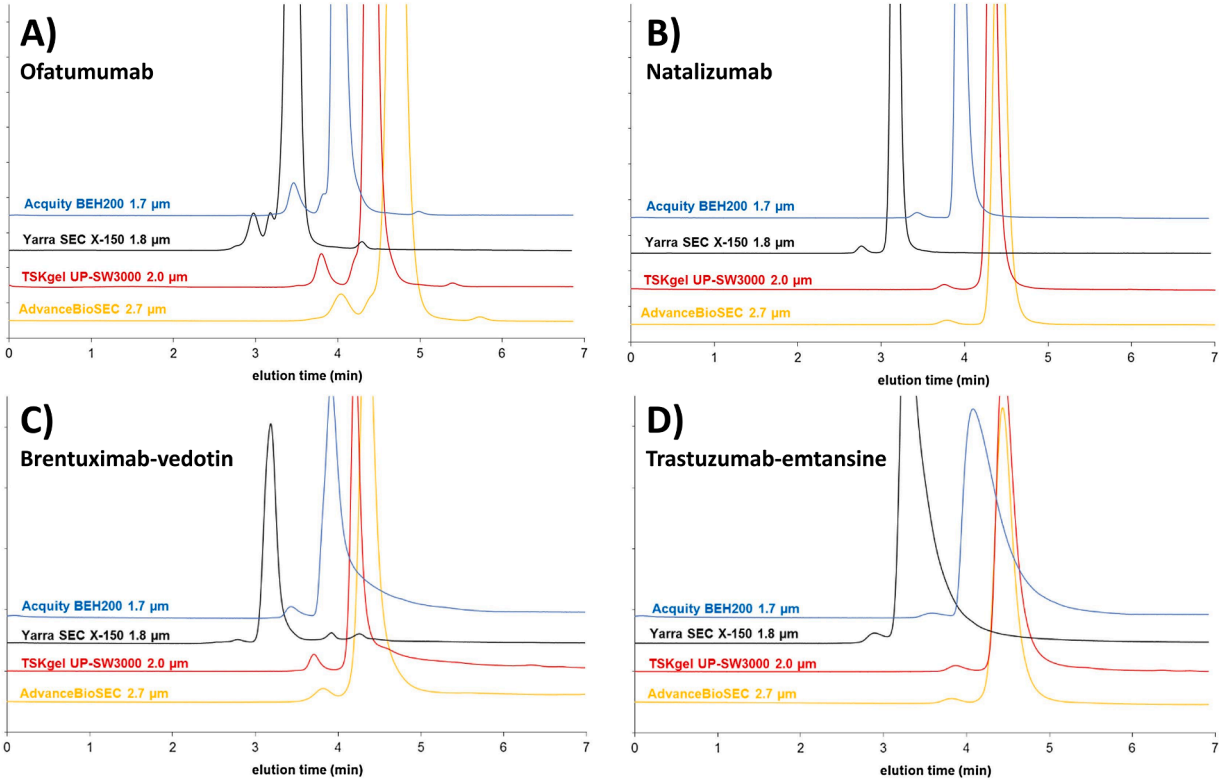

Fig. 2. Comparative overlaid representative chromatograms observed on the different columns for ofatumumab (A), natalizumab (B), brentuximab-vedotin (C) and trastuzumab-emtansine (A). The mobile phase contained 100 mM disodium hydrogen-phosphate buffer and 200 mM sodium chloride in water, pH = 6.8 at 25 °C. Columns were operated at F = 350 μL/min. Adapted with permission from [40].

regardless of the column used. The robustness of modern SEC columns packed with 1.7 μm particles has also been recently investigated. Due to the inherent fragility of large pores particles and repeated exposure to different analytical conditions, the lifetime of a SEC column is typically limited to less than 500 injections [41]. In this work, the authors have evaluated 19 columns of the same type (BEH 200 Å 1.7 μm Columns) using a proprietary mAb produced at Regeneron. System suitability parameters, such as USP resolution, USP plate count, USP tailing factor, elution time, peak width, and peak height, were used to evaluate SEC column performance. A general linear model was constructed which revealed that elution time, peak width, and USP tailing factor increased with the number of injections, while peak height, resolution, and plate count decreased with the number of injections. After 1000 injections, USP tailing factor and peak width increased by more than 10%, while resolution and plate count decreased by more than 10% compared to their initial values. Today, a variety of SEC columns are available that are packed with sub-3 μm particles, as they are widely used for the analysis of mAbs and related compounds [42,43]. In addition to particle size considerations, it is important to note that modern SEC columns have also significantly reduced column volumes compared to a classical 300 × 7.8 mm column dimension. In fact, due to improved efficiency, it is possible to reduce the length to 150 mm, while maintaining appropriate kinetic performance. The shorter column allows faster analysis, and reduces the pressure generated by the packing. In addition, a column diameter of 4.6 mm is commonly used in modern SEC columns. This allows an analyst to further reduce sample and mobile phase consumption. However, due to the large reduction of the column volume between classical and modern SEC, by approximately 6-fold, it is necessary to optimize the chromatographic instrument to limit system-related band broadening.

In SEC, the analytes are typically partially excluded from the pores with ideally no adsorptive interaction with the packing material. This means analytes will exhibit very low retention factors (k') generally ranging between −1 and 0. This leads to an inherently low column band variance, emphasizing the need to work with a fully optimized system [36,44].

A recent evaluation of instrument compatibility (i.e. regular HPLC, non-optimized UHPLC, and carefully optimized UHPLC) with modern SEC columns (150 × 4.6 mm, sub-3 μm particles) showed that apparent efficiency is very significantly influenced by the instrument configuration and its disposition [36]. For example, the analysis of mAb samples on a regular HPLC system with an extra column volume (ECV) of 65 μL resulted in a severe loss of efficiency (approximately 60 - 85%). To use these columns more effectively, optimized UHPLC systems with ECV below 10 μL are essential. In some extreme cases, columns packed with sub-2 μm particles may even have lower apparent efficiencies than those packed with larger particles (3 - 5 μm) when using conventional HPLC systems. This situation is obviously counterproductive. In addition to the instrument volume, the material used for the connecting tube also influences the kinetic performance of a modern SEC separation. In fact, PEEK lined tubing has been shown to be more beneficial than stainless steel tubing, as it minimizes protein adsorption, leading to an apparently higher plate count (typically 10 – 15% higher on average) [44].

In conclusion, modern 150 × 4.6 mm SEC columns packed with sub-3 μm particles offer improved efficiency and faster separation, and they have now been adopted into routine analysis of biopharmaceuticals. It is essential, however, that they are used with optimized UHPLC systems.

3.2. The importance of the hydraulic diameter of a packed bed

An important characteristic of a SEC column is the interstitial distance between the particles of the packed bed. Various measures exist to describe this characteristic length such as hydraulic radius (r_c), hydraulic diameter (d_h), intraparticle channel size, "equivalent spherical diameter", "contact diameter" or "sub-channel" size [45–47]. In SEC (and other chromatographic modes), knowing the d_h is important to estimate and minimize the interstitial shear rates to which the analytes are subjected during their passage through the column [48,49]. Fig. 3 shows a schematic view of the hydraulic radius and diameter as the interstitial distance between spherical particles.

For very short d_h distances, it is hypothetically possible for analyte degradation and sieving to occur in the interstitial medium. When degradation occurs, it is often referred to as "flow induced" degradation [48]. It may seem that such degradation can also occur through column frits, since the frit pore size is typically smaller than the size of the packed particles. However, it has been shown that frit-induced sample degradation is less significant compared to on-column degradation, probably due to the very short passing time of the analytes through the frit. Nevertheless, direct frit-induced degradation remains an area of interest for future study [50].

In a well-packed column, the hydraulic diameter is determined by the interstitial porosity (ε_i) and the particle size (d_p) [45,46,51,52]. A smaller d_p and a lower ε_i (denser packing) will result in a smaller hydraulic diameter. The hydraulic diameter directly determines the shear rate (and these terms are inversely proportional) [49]. Therefore, particle size and column porosity have important effects on SEC separations, as they both determine the column pressure and the shear rate. Thus, even though smaller particles usually result in higher column performance, there is a theory-driven concern that excessively small particles (i.e. $d_p < 2$ μm) should not be applied to the analysis of lipid nanoparticles (LNPs), adeno associated viruses (AAVs), virus like particles, and large nucleic acids. However, it should be kept in mind that not even modern packing materials exhibit a discretely narrow particle size distribution. The polydisperse nature and range of particle sizes within a packed column should be considered when modeling the theoretical limits of SEC and its applicability to different-sized analytes. The size of LNPs ranges between 60 – 250 nm (hydrodynamic diameter), [53] though COVID-19 vaccines exhibit a narrower range of LNP sizes; 92.89 ± 2.53 nm for Pfizer (Comirnaty™ (COVID-19 Vaccine, mRNA)) and 93.00 ± 3.00 nm for Moderna (Spikevax™ (COVID-19 Vaccine, mRNA)) [54]. To avoid any restricted passage through the intraparticle channels, the hydraulic diameter of the packing should be at least 2 - 3 times larger. Such d_h values correspond to 1.5 – 2.1 μm column particles. Based on theory, one can thus conclude that it could become problematic to attempt intact LNP analyses with sub-2 μm packing materials.

Fig. 4 shows the hydraulic diameter of packed beds as a function of a column's interstitial porosity. Calculations are provided for columns packed with uniformly sized 1.5, 2.5, 3.5 and 5 μm particles. As an

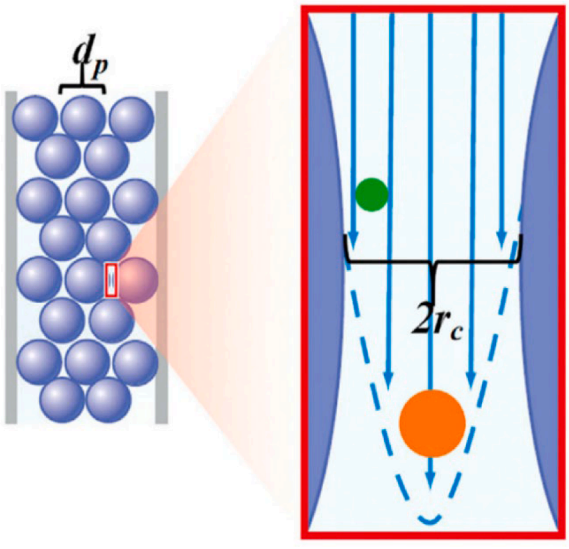

Fig. 3. Schematic view of the hydraulic diameter ($2r_c = d_h$) in a column packed with d_p (particle diameter). Adapted with permission from [45].

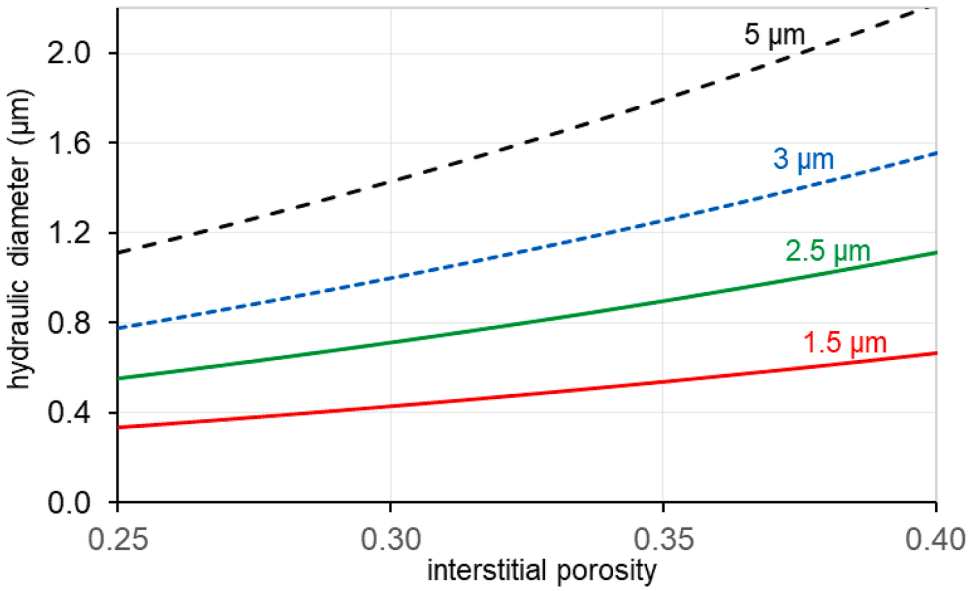

Fig. 4. Plot of hydraulic diameters as the function of interstitial column porosity, assuming uniform 1.5, 2.5, 3 and 5 µm particles. (Unpublished data from the authors, see SI for details).

example, a column packed with 2.5 µm particles will result in $d_h = 0.75 – 1.0$ µm when considering ε_i between 0.30 and 0.37 (which is a typical porosity range of commercial SEC columns). Regarding shear forces, a 1.5 µm column results in 1.7- and 3.3-times higher shear rates than a 2.5 µm and 5 µm packing, respectively - when operated at the same flow rate.

3.3. Selection of the optimal pore size

A packing material's average pore diameter (d_{pore}) and pore size distribution (PSD) is critical to achieving an optimal separation. To avoid restricted pore diffusion, the average d_{pore} should typically be approximately three times larger than the target analyte size [55]. Thus, from the point of view of kinetic efficiency, a large pore diameter is advantageous. If the pores are too small, the concentration of an analyte in the pores may reach equilibrium slowly (resulting in peak broadening or tailing) [56]. On the other hand, a pore size that is too large may not discriminate between similarly sized analytes, resulting in poor selectivity. The highest selectivity is expected when the equilibrium constant (K_{SEC}) is about 0.5. This is when the analyte comes to elute in the middle of the elution window and when the target analyte enters half of the internal pores [29].

To estimate the size or molecular mass of an unknown analyte, calibration curves are often used in SEC. To create a calibration curve, a set of compounds having different masses or sizes (i.e. homologue series, protein/oligonucleotide ladder…) are injected and the molecular mass (or its logarithm) of the analytes is plotted against the observed elution volumes [57–59]. In turn, the SEC calibration curve essentially transforms the PSD of the column's accessible pores [58]. For the sake of simplicity, one can visualize spherical molecules passing through single-sized homogeneous tubular pores. It is reasonable to assume that if the hydrodynamic diameter of the solute is smaller than the meso-pore diameter, it will enter the pore. Otherwise, it will be excluded. Knowing the average d_{pore} and PSD (or variance of the distribution) allows the estimation of the exclusion rate of a solute with a given hydrodynamic diameter [60]. Therefore, calibration curves can be directly estimated from the pore size distribution of the packing material [58].

Fig. 5 shows three different PSD materials and their corresponding calibration curves. The left end of the calibration curve is related to total exclusion (or interstitial porosity). The right end of the calibration curve is determined by the total porosity (or total permeation) of the packing material.

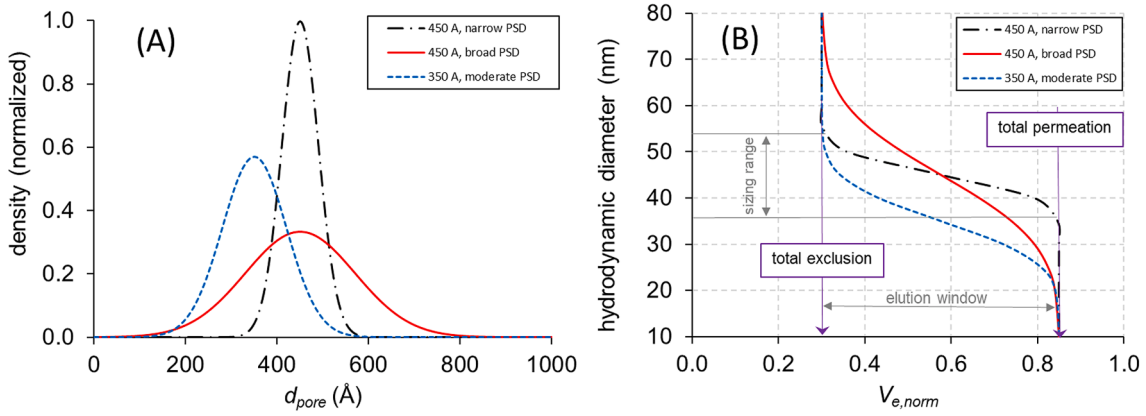

Fig. 5. Pore diameter distribution plots (A) and the corresponding (expected) calibration curves (B). d_{pore} is pore diameter and $V_{e.norm}$ refers to the normalized elution volume. (Unpublished data from the authors, see SI for details).

The elution window between the exclusion and permeation limits is often referred to as the "useful elution window", "fractionation range" or "sizing range" of the column. Very often, linear or polynomial fits are used in this window of the calibration curve to describe the proportionality between solute size and mass as well as elution time and volume [57]. The slope of the calibration curve is a consequence of the PSD, while the vertical position of the curve is determined by the mean pore diameter. A narrow PSD results in a flat calibration curve and therefore high selectivity. However, its sizing range is limited. In contrast, a wide PSD results in a steeper calibration curve and therefore lower selectivity and a wider sizing range. A decrease in the mean pore diameter shifts the calibration curve downward and therefore a smaller pore diameter is better suited to the separation of smaller analytes. Each of these effects is illustrated in Fig. 5. Note that the PSD of wide-pore materials tends to broaden as the average pore diameters becomes larger (as a stochastic consequence of standard pore enlargement techniques)

Based on a review of current literature review and our experience, we have come to prepare pore size recommendations for several common large molecules. These are summarized in Table 1 [22,34,40,61–63].

Note: the compounds used to construct a calibration curve must resemble the target analytes in shape, physicochemical nature, and size. Molecular shape (e.g. circular, linear) and flexibility (i.e. tendency to stretch or unfold during migration through the column) are particularly important [64]. Today, several SEC calibration kits are commercially available from different suppliers, including different protein ladders (suggested for different column pore sizes) and nucleic acid ladders (such as ssDNA 20 to 100 mers and dsDNA 50 to 1350 mers).

3.4. Column coupling to expand sizing range and adjust selectivity

In some cases, both low- and high-molecular-weight species must be separated. It is possible that a single column of a given morphology will not provide adequate selectivity for both small and large analytes. A possible solution is to couple two or more columns in series to extend the size range of the separation [65,66]. A practical advantage of a multi-column system is that the pore size distribution of the column can be easily adjusted by combining different lengths of different mesopore structure segments. Gritti reported a theoretical study on the tunable morphology of a tri-column SEC system, considering different combinations of 3, 6 and 9 cm individual column segments of three different morphologies [67].

From the point of view of selectivity, the order of the individual column segments is irrelevant as the same selectivity is expected for a time-invariant SEC separation mechanism [60]. However, an important consideration is the stability of the packed bed. Since packings with small pore sizes are mechanically more stable than materials with large pore sizes, columns must be connected in order of increasing pore diameter. Columns packed with the most "fragile" particles could deteriorate if placed in the upstream position. Placing them in the downstream position protects them from potential bed collapse because the sudden pressure changes caused by the injection process are largely absorbed by the column immediately after the injection valve [67].

The length of the individual column segments does impact selectivity and therefore needs to be optimized. The contribution of the individual columns to the overall elution time/volume is additive. It can therefore be easily calculated and modeled. The same optimization procedure used for "phase optimized liquid chromatography" can be applied [68,69]. The elution times/volumes and peak variances of the different analytes must be measured for all individual column segments. These values can then be used to calculate the optimal stationary phase composition.

The only drawback to the column coupling approach is that a multi-column system often results in a non-linear calibration curve. In these cases, a higher order polynomial fit is advantageous, resulting in less error in the evaluation of the mass/size of unknown analytes [65]. To overcome this difficulty, single columns packed with a carefully designed mixture of two or more different pore sizes and distributions (e.g. mixed bed columns) are available to provide a nearly linear calibration curve. In addition, optimized packing technology was developed in which SEC packings consist of layers of different, tightly controlled pore sizes.

Fig. 6 shows some model (derived from calculations) chromatograms expected on a 200 Å (30 cm), 400 Å (30 cm) and coupled 200 + 400 Å (15 + 15 cm) columns for a mixture of five compounds (in the hydrodynamic radius range of 120 – 230 Å). The 200 Å column alone provides poor selectivity for the largest analytes (peaks 1 and 2 co-elute), but high selectivity was obtained for the smaller analytes. In contrast, the 400 Å column provides high selectivity for the large analytes but low selectivity for peaks 4 and 5 (partial separation). The tandem column system (equivalent length of 200 and 400 Å segments) results in adequate selectivity for all peak pairs.

3.5. Importance of secondary interactions

Ideally, an SEC separation is an entirely entropic process based on differential filtration of analytes with varying hydrodynamic radius through the pores. As such, no physico-chemical interactions with the packing material are desired. However, in practice, this is difficult to achieve since biopharmaceutical molecules contain a multitude of functional groups capable of various types of interactions, ranging from: electrostatic and hydrophobic interactions to H-bonding [30]. Although most of these contacts *via* a single residue are weak, biomolecules often display sizeable surface areas and patches of concentrated moieties that can exacerbate secondary (or non-specific) interactions even for carefully designed SEC columns. These effects are expected to be more pronounced with the growing molecular size and complexity of emerging biotherapeutics. One could predict that adapted surface technologies and method development approaches will be needed to address this challenge. Recently, this was highlighted in the case of irreproducible routine SEC characterization of foot and mouth disease virus, used in vaccines, where different columns lots engaged the analyte to a different degree and extensive optimization of method conditions was required to eliminate column batch variability [70].

Charged patches are often present on protein surfaces and nucleic acids are inherently anionic due to their phosphate backbones [71]. The chance to encounter for problematic electrostatic interactions with these analytes is high. This can mean ion exclusion and ion exchange effects depending on the relative polarity between the species and column components. In each case, elution time and peak shape can be impacted [72]. Moreover, a pronounced adsorptive interaction often leads to problematic recovery issues, especially for high molecular weight species (HMWS) [73]. This is also evident during the analysis of negatively charged analytes which are known to readily adsorb to stainless steel [44,74]. Recent efforts to mitigate this effect from column hardware are discussed in Section 3.2. On the other hand, many therapeutic antibodies are basic, with pI > 7.5, which means that they carry a net positive charge when analyzed under standard conditions at physiological pH [75]. Such molecules can readily interact with low abundance negative charges found in silica based packing materials [76].

Table 1
Recommended average pore diameter for some typical applications.

analyte	proteins, MW ≈ 15–80 kDa	mAbs, ADCs	AAVs	large PEGylated proteins	LNPs, plasmid DNA
average pore size	150 – 200 Å	200 – 300 Å	450 – 500 Å	500 – 1000 Å	1000 – 1500 Å

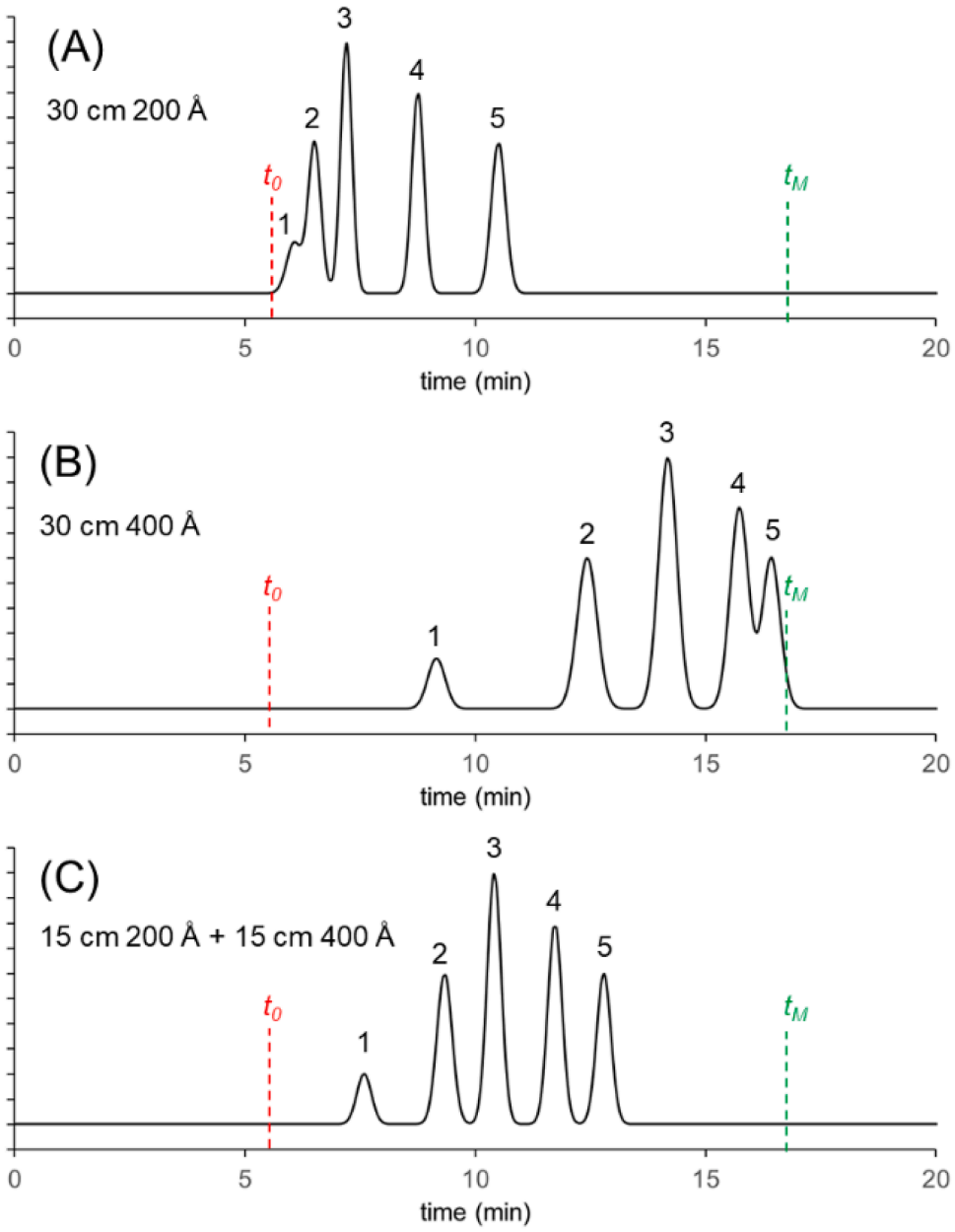

Fig. 6. Model chromatograms to illustrate the benefit of a tandem column system. Total column length: 30 cm, column diameter: 4.6 mm, column's total porosity: 0.85, interstitial porosity: 0.30, flow rate: 0.25 mL/min. Mean pore diameters: 200 Å (A), 400 Å (B) and 200 + 400 Å (C). Normal symmetrical distribution was considered for the PSD with σ = 60 Å. Hypothetical analytes' hydrodynamic radius: 23 nm (peak 1), 19 nm (peak 2), 16 nm (peak 3), 14 nm (peak 4) and 12 nm (peak 5). (Unpublished data from the authors.).

Some biopharmaceuticals display "greasy" regions on their surfaces which may interact with certain hydrophobic sites of the nominally hydrophilic packing material. These could be created via bonding chemistry, end-capping, and cross-linking with organosilane reagents, used to reduce silanol activity and increase stability of the particles [77]. Such interactions can also significantly impact chromatographic performance with delayed elution time (beyond t_M) as a frequent symptom [72,78]. These can be pronounced for ADCs conjugated with lipophilic payloads [79].

Generally, the above-described impact of secondary interactions can be limited by the use of sufficient concentrations of additives in a mobile phase. It is the role of an SEC method developer to screen for and weaken the secondary interactions between the analyte and column components. Typically, one employs salts (usually sodium or potassium with the latter being more efficient) for electrostatic interactions and organic solvents (usually methanol/isopropanol or acetonitrile) [38,79]. Other effects from adjusting the mobile phase with zwitterionic and mild chaotropic additives are also worth exploring. These types of additives are amino acids, such as arginine, lysine and anions, such as perchlorate or thiocyanate [70,80,81]. However, this strategy may impact analyte (higher order) structure and introduce other undesired artefacts and normally requires validation with orthogonal methodologies [82]. Finding optimal conditions could also be a laborious and non-straightforward process. For example, an increase of mobile phase ionic strength limits the effect of electrostatic interactions, but it also directly enhances the strength of hydrophobic interactions [72,80]. Thus, successful method development may require balancing many parameters and can be best realized via automation (further discussed in Section 2.6) and design of experiment (DoE) approaches [78,83].

Alternatively, SEC column providers have been working on

optimizing the surfaces of their packing materials [84]. For example, diol bonded particles were once state of the art but have recently been shown to exhibit secondary interactions with challenging analytes when compared to newer hydroxy-terminated polyethylene oxide (HO-PEO) bonded materials [77].

A recent systematic SEC column comparison against a diverse subset of 12 antibodies confirmed that the HO-PEO bonded stationary phase in combination with low adsorption hardware yielded minimal secondary interactions with the analytes [72]. As the result of a rigorous DoE SEC method development procedure, a generic platform SEC method was established for antibodies. In general, with these low adsorption SEC columns, it is reasonable to start method development with a standard 1x strength PBS buffer. The influence of secondary interactions can then be tested with KCl and organic solvent according to the decision tree shown in Fig. 7. A corresponding DoE method development approach is discussed in Section 2.6.

Further optimization of packing materials for the analysis of biopharmaceuticals and further progress on low adsorption hardware will facilitate establishing platform SEC methods for an even broader array of biotherapeutics.

3.6. Automated method development

Various systematic method development approaches have been reported for SEC separations [34,38,40]. The critical steps of the method development process are well established. These include the selection of appropriate pore size for selectivity, finding the right mobile phase composition to avoid non-specific interactions, and the optimization of flow rate and column length to achieve high separation efficiency in a reasonable time. Here, we focus only on aspects of automation and evaluation.

In SEC, as there is no analyte retention, common retention modeling approaches do not apply. Therefore, instead of the often-used semi-empirical models, factorial designs of experiments (DoE) seem to be more appropriate to study the effects of the most relevant factors. For SEC, those factors are the mobile phase ionic strength, mobile phase organic modifier concentration, and mobile phase/column temperature [83]. The responses to be studied should be carefully selected. It has been proposed that the most meaningful responses are (1) the resolution between monomer and HMWS, (2) the observed HMWS% (recovery) and (3) the width of the main peak (i.e. monomer) [85]. By studying these factors and responses, both electrostatic and hydrophobic secondary interactions can be explored, understood, and ultimately mitigated.

Most chromatographic modeling software (DryLab™ Software (Molnar Institute), Fusion QbD™ Software (S-Matrix), ChromSwordAuto Software (ChromSword), AutoChrom™ Software (ACD Labs)) support direct communication and full control between the modeling software and the instrument controlling chromatographic data system (CDS) [86]. These software packages can fully automate the method screening and optimization procedure [87]. Once the appropriate DoE is selected in the modeling software, all the instrument method parameters, method sets and sample set parameters can be quickly set within the modeling software (including column equilibration times, washing steps, repetitions, and blank injections). Then, the whole experimental design and corresponding instrument parameters created in the modeling software can be transferred to the CDS. Once the experiments are performed, all measured data required to build up the model (e.g. chromatograms, retention times, peak areas, peak widths, peak symmetry) can be directly sent from the CDS to the modeling software, and the models can be quickly set up. After selecting a robust working point from in-silico optimization the corresponding conditions and method parameters can be transferred again to the CDS in order to automatically perform the experimental verification of the selected working point [83].

Most modeling software is now capable of identifying conditions (the working point) where all method requirements (i.e., all responses) are satisfied. This is done by superimposing the various responses and graphically visualizing the method criteria. This approach is often called Multiple Attribute Modeling (MAP). This MAP approach is particularly

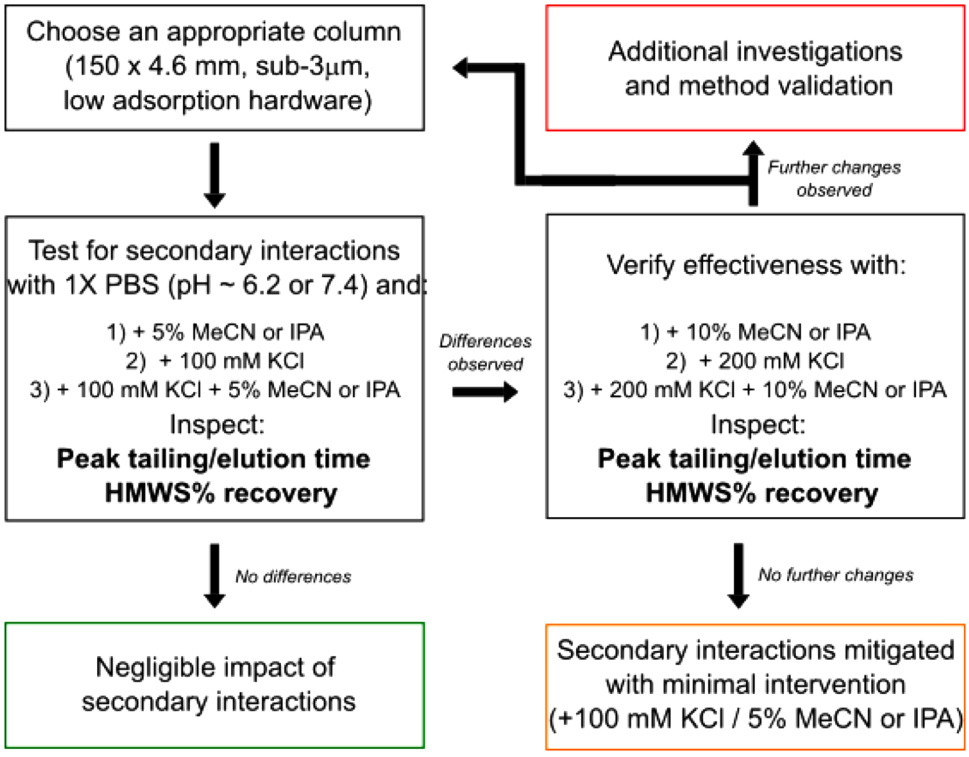

Fig. 7. Simplified method development decision tree aimed at verifying the impact of secondary interactions on an SEC separation. The proposed conditions were adapted from those commonly found in literature [40,77] for assessing the impact of secondary interactions.

interesting for SEC, where not only the resolution but also the recovery is strongly influenced by the method parameters.

The above discussed fully automated procedure has been applied for the SEC analysis of two mAbs used to treat COVID-19, namely casirivimab and imdevimab [83]. The automation module of the DryLab Software was used to automate the experiments. Simultaneous effects of critical method factors were evaluated using a simple full factorial design. Three response functions were examined. The results indicated that secondary interactions were practically negligible in the range of method factors studied. The resolution between HMWS and monomer peaks was found to be higher than 1.5, indicating that the pore size of the packing material was properly selected (250 Å).

Although method development approaches for SEC separations are well documented, the authors believe that most practicing chromatographers still rely on trial and error and other time-consuming procedures. We encourage chromatographers to use automation and modeling tools to shorten, understand and properly document their SEC method screening and development processes.

3.7. Combination of SEC with MALS to gain more information on the sample

Multi-angle light scattering (MALS) detectors complement optical detectors like refractive index (RI), tunable ultraviolet (TUV) or photo diode array (PDA) that are more commonly applied to detect analytes eluting from an SEC separation. MALS provides both chemical information such as molecular weight (MW), size, aggregation, and the distribution of each species in a fractionated sample, as well as biophysical attributes such as conformation, and the type of higher order structure (i.e. oligomeric state). The accuracy of this detector is closely related to the number of angles that are measured as well as the mathematical corrections made to account for intramolecular interference, which increases with the analytes size. More sensitive detectors with 18 angles can determine MW in the range from 200 Da - 1 GDa [88].

In addition to MW, a MALS detector also provides the particle's size, specifically the radius of gyration (R_g) or root mean square radius (rms) for analytes from 10 to 500 nm [88,89]. Integration of the mass - distribution which includes multiple scattering centers and radii, produces R_g [90]. Through additional mathematical models or using the relationship of the log R_g vs log MW, the molecular conformation can be uncovered.

Online or embedded dynamic light scattering (DLS), or quasi-elastic light scattering (QELS) is commonly included with advanced MALS detectors. This additional type of light scattering enables quantification of the hydrodynamic radius (R_h) for analytes as small as 0.5 nm in radius, which extends the lower end limit of a standard detector [88].

Furthermore, when run at multiple concentrations, MALS assays offer additional insights into a molecule's stability through the second virial coefficient (A2). This coefficient indicates whether there is attraction (A2 < 0) or repulsion (A2 > 0) among the analytes [89]. This type of insight is helpful when considering the long-term stability of a biotherapeutic.

SEC-MALS is a versatile technique widely applied in various biologic scenarios. It covers a broad range of applications, from the conventional analysis of protein aggregation and oligomeric determination to measuring the extent of conjugation and the empty/full ratio of viral vectors such as AAV and LNP as well as their genomic titer [88,89,91–94]. What sets SEC-MALS apart is its calibration-free nature and its effectiveness in accurately assessing non-globular-shaped samples, providing precise molecular weight and species distribution information for complex samples. Another notable advantage is its capability to dissect the contents within an eluting peak, enabling the evaluation of SEC separation quality. Specifically, SEC-MALS excels in revealing polydispersity within a single eluting peak or identifying the content of a shoulder as with a LMWS peak. MALS also excels in accurately assigning molecular weights to proteins that, due to various configurations or secondary interactions, elute at volumes inconsistent with their actual molecular weight. Fig. 8 illustrates this phenomenon, where three mAb samples with similar molecular weights elute at different volumes [88]. This discrepancy can arise from factors such as potential hydrophobic/ionic interactions with a column or a non-globular configuration of the protein. Additionally, post-translational modifications and other alterations like PEGylation may extend the hydrodynamic radius, leading to earlier elution without significantly impacting the molecular weight [88,89].

SEC-MALS offers the added advantage of providing detailed information about the components within an eluting peak. This is particularly valuable for complex samples, including glycosylated proteins or those modified with additional linkers and drugs [92]. Its effectiveness increases with the complexity of the samples. Notably, SEC-MALS is exceptionally well-suited for analyzing samples like ribonucleoproteins (RNPs), antibody oligo conjugates (AOCs) or ADCs. A recent study using native SEC-MALS on SARS-CoV-2 nucleocapsid protein found a molecular mass of 99.9 kDa, which was similar to results obtained from other techniques, demonstrating the excellent reliability of this technique [95]. Regarding antibody oligonucleotide conjugates, a study utilized SEC-MALS to confirm the uniformity of fullerene-based spherical nucleic acids that were linked to antibodies where the results demonstrated that the overall molecular weights obtained using SEC-MALS closely matched the expected theoretical values [96]. SEC-MALS has also been

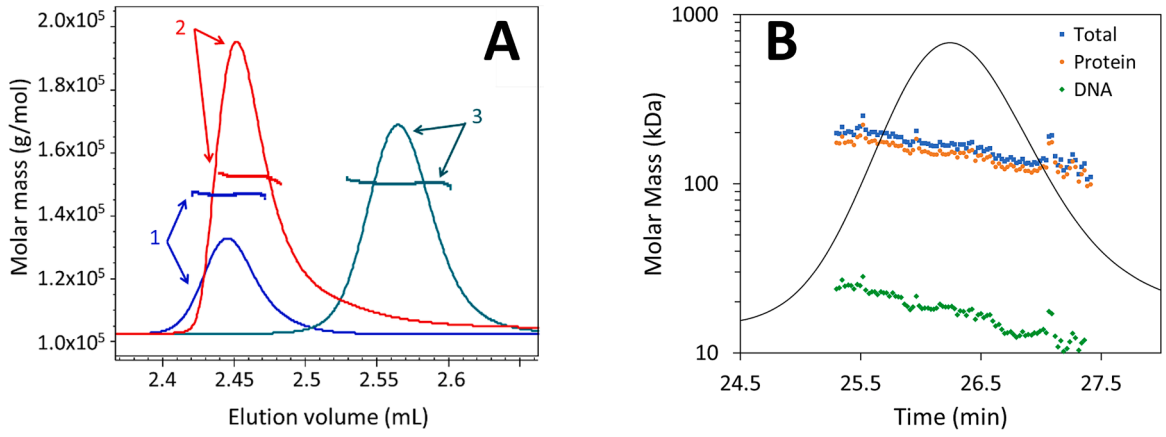

Fig. 8. (A) Elution profiles of several different mAbs with similar molecular weights eluting at different times (Solid UV trace) but identified as having the same molecular weight by MALS. (B) Contents of a single eluting peak, UV chromatogram, solid line, deconvoluted into the mass values of proteins, DNA and the Protein-DNA complex through MALS analysis. Adapted with permission from [88].

used in biosimilarity assessments with respect to stability by characterizing aggregates between different mAbs [97]. In a separate study, it was observed that SEC-MALS was superior to other orthogonal techniques and displayed strong correlation with SV-AUC values of AAV particles ranging from full to empty. Furthermore, SEC-MALS results were consistent with ddPCR and ELISA measurements pertaining to both vector and capsid titers. SEC-MALS not only maintained high levels of linear accuracy and precision, but also achieved quality control recommendations for chromatography. When compared to other assays that indicate stability, SEC-MALS performed comparably well to ddPCR, capsid ELISA, and infectivity assays under accelerated stress conditions [94].

Finally, it is important to note that a MALS detector does not replace other optical detectors; rather, it is essential for determining the concentration used in the model equation for molecular weight determination. In the case of complex samples, both a UV and RI detector are crucial to deconvolute the total molecular weight into its components, such as protein titer, nucleic acid titer, or the drug-to-antibody ratio. The combination of MALS with fractionation by SEC is crucial for gaining a fundamental understanding of a sample and ensuring thorough biomolecular characterization. This is applicable not only to standard samples where clarity on "what is under the peak" is desired, but also to complex non-globular samples.

4. Recent advances in SEC

4.1. Narrow-bore and micro-bore SEC columns

Recent trends in the pharmaceutical and biotechnology industries call for the miniaturization of SEC separations. More robust and more sensitive SEC techniques are needed to reduce sample consumption and improve hyphenated MS capabilities. For these reasons, there is a need to decrease the diameter of SEC columns (down to 2.1 and 1 mm ID) and to work towards the optimization of their use.

However, due to the nature of the SEC elution mechanism, the retention-related term of the column peak variance (CPV) is extremely low. The consequence of this is that extra-column dispersion (ECD) can significantly impact apparent column efficiency, as previously discussed [36,98]. On the other hand, CPV is also proportional to the column volume. Hence, smaller column volumes will result in even smaller CPV. The only way to compensate and provide adequately large CPV is to increase the column volume. As such, larger volume columns can improve the apparent efficiency [34].

There is a contradiction here: there is a need for small column volumes, but small columns suffer from ECD. Only a few pieces of work have been published on the use of narrow- and micro bore SEC columns. The effect of SEC column diameter on the detection of proteins and their aggregates was systematically studied by Eksteen. When comparing 4.6, 2 and 1 mm ID SEC columns, it was found that detection sensitivity drastically increased with the decrease of column ID. Capillary SEC columns (300 μm ID) appeared to be particularly promising for improving the sensitivity of antibody fragment analysis and facilitating the analysis of very small amounts of samples [99,100].

A microflow SEC column (50 × 1 mm) was applied to achieve subunit separations and analyze non-covalent protein complexes using native MS conditions [101]. Coupling of such a 50 × 1 mm SEC column to multichannel microflow emitters resulted in 10 to 100-fold gains in MS sensitivity. However, it was noted that extra column tubing and dispersion effects significantly constrained the observed chromatographic performance of the 1 mm ID column. Therefore, if SEC chromatographers want to miniaturize sizing separations to a column diameter $\leq$ 1 mm, there is more work to be done on chromatographic instruments and flow paths.

In a recent report, the potential of a 2.1 mm ID SEC column was studied and compared to a reference 150 × 4.6 mm SEC columns [102]. This study reaffirms the importance of very low system dispersion for SEC separations. At the same time, it shows that a very efficient 150 × 2.1 mm SEC column can offer a balanced compromise between apparent separation efficiency, sample consumption and MS compatibility. An apparent efficiency close to 50% of the 150 × 2.1 mm column's theoretical efficiency can be achieved on a commercial UHPLC system.

On another note, it should be mentioned that the intrinsic efficiency of modern SEC columns has probably been underestimated in the past due to additional band broadening caused by non-specific interactions between solutes and the column hardware (especially column frits). The use of low adsorption column hardware has made it possible to measure lower column dispersion values, which in turn resulted in more accurate modelling of SEC columns intrinsic efficiency.

4.2. Low-adsorption ("bioinert") SEC column hardware

Undesired secondary interactions are particularly problematic for SEC separations. Column hardware can be a source of these secondary interactions [77]. Only recently was the adsorptive loss of certain negatively charged analytes to stainless steel surfaces systematically studied. These metal elements can be found not only as part of the column hardware (housing/frits) but also throughout the flow path of chromatographic instrumentation [103]. Various solutions were evaluated showing that the replacement of the base material (for titanium or nickel-cobalt alloys) as well as use of chelators (e.g. medronic acid, ethylenediaminetetraacetic acid etc.) in the mobile phase offered improved performance but did not completely mitigate the adsorptive effect. It was also shown that analyte conditioning is temporary. Instead, the problematic surface can be masked with a protective layer [104]. The polyether ether ketone (PEEK) surface have been widely employed to improve recovery and chromatographic performance. However, it is recognized that PEEK is not optimal for all cases. Certain analytes can experience increased absorption to PEEK, because of its hydrophobicity [105]. This can pose a particular challenge in the context of aqueous SEC analyses of increasingly larger biopharmaceuticals and their aggregates. For similar reasons another chromatographic surface (HST, hybrid surface technology), based on vapor deposited hybrid silica with exposed ethylene bridges and incomplete capping of silanols, was deemed to not be perfectly optimized for SEC separations [103]. To adapt this technology for aqueous chromatography, this base layer was hydrophilically modified. Columns constructed with this hydrophilic hybrid surface (h-HST) hardware exhibited superior performance when it came to HMWS recovery and peak shape [106]. The benefit was attributed to a reduction in both electrostatic and hydrophobic secondary interactions. Other manufacturers have also introduced columns with low-adsorption coatings, but they were not designed explicitly for aqueous separations. An overview of currently available "bioinert" SEC columns can be found in Table 2 (columns which do not specify the details on the low-adsorption hardware were not included). A recent study of SEC columns has confirmed the key role of the h-HST modification: an h-HST

Table 2
Overview of low-adsorption SEC columns and used technology currently available on the market. Technical specifications (hardware and/or frit material) were taken from publicly available sources on manufacturers' websites or brochures.

Manufacturer	Column Example	Technology	Details
Waters	XBridge Premier BEH SEC	h-HST	C, O hydrophilically modified ethylene-bridged hybrid surface
Phenomenex	Biozen SEC	BioTi	Titanium lining and frit
Tosoh	TSKgel BioAssist SEC	PEEK	PEEK housing
Sepax	Zenix and SRT SEC	PEEK	PEEK housing
YMC	YMC-Pack Diol SEC	PEEK	PEEK lining and frit
Agilent	AdvanceBio SEC	PEEK	PEEK lining and frit

column was found to be the most effective, among various comparison columns, at minimising analyte interactions [72]. It is expected that with growing complexity of the biopharmaceuticals the use of low adsorption hardware technology will become more and more essential for successful SEC separations.

4.3. Ultra-wide pore SEC columns for large molecules

As discussed in section 2.3, many new modalities and their aggregates are significantly larger in diameter than mAbs. This requires the use of a column with sufficient pore size to match their hydrodynamic radii. Depending on the exact biotherapeutic product, these molecules can have diameters ranging from 100 – 600 Å for molecules like AAV vectors to 600 – 2500 Å for LNPs [53] and >1000 Å for plasmids, adenovirus and lentivirus [107–110]. Meanwhile, mRNA can exhibit a range of diameters correlated with their length. A 1000 nucleotide long mRNA has a R_g of approximately 15.6 nm, while the R_g of a 4000 nucleotide mRNA is about 25.2 nm [111]. Suitable SEC columns have long been available in 5 µm or larger particles of various nominal pore sizes ranging from 300 to 2000 Å. On the other hand, modern SEC columns with smaller particles (sub-3 µm) from most manufacturers reach only "wide pore" size of 300 Å, with a few notable exceptions (currently commercially available): Waters XBridge™ Premier GTx 2.5 µm, 450 Å SEC Column (see Fig. 9 for SEM image of the stationary phase and pore size distribution), dedicated for gene therapy applications due to the use of hydrophilically modified (h-HST) hardware, and older generation columns: Phenomenex Yarra™ SEC-4000 3 µm, 500 Å Column and Shodex PROTEIN KW403–4F, 3 µm, with a 800 Å maximum pore size [61].

A recent report suggested that newly developed columns with "ultra-wide" pores (>500 Å) are in the process of entering the market, as prototypes of efficient 3 µm SEC columns with nominal pore size of around 1300 Å have been demonstrated to be useful for the analysis of various new modalities (i.e. mRNAs, LNPs, and plasmids) [22].

While many older generation ultra-wide pore columns can be repurposed for the analysis of biopharmaceuticals, it is imperative to consider the suitability of the packing material and column hardware for the analysis of such molecules. If a method is developed haphazardly, an analyst might encounter analyte loss and resolution challenges with batch-to-batch or lot-to-lot column changes [106]. The other consideration for such columns is their mechanical strength and their compatibility with MALS detectors. Ultra wide pore silica can suffer from poor stability, especially with the decreasing particle size, [67] which may cause residual shedding leading to unacceptable noise levels for sensitive light scattering detectors or lengthy conditioning procedures [112].

Increased availability of sub-3 µm particle, high recovery and MALS compatible ultra-wide pore SEC columns are expected to enable and promote detailed characterization of new modalities. Their increased efficiency will be the key to expediting the development and release testing of complex molecules. However, it should be noted that SEC technology might not be ideal > 2000 Å complexes due to technical limitations and physical constraints. Sizing separations, which do not use packed particle beds, such as A4F, might be more suitable due to the absence of shear forces and filtration effects as well as the potential for superior recovery.

4.4. Recycling SEC

Achieving enhanced resolution in SEC analysis is challenging due to the fact that selectivity is driven almost exclusively by the mean pore size and pore size distribution of the column. So, the only parameter that has an impact on resolution and can be improved is efficiency. As discussed in sections 2.1. and 2.2., reducing particle size is an attractive option to increase resolution, but this also leads to increased pressure and stronger shear forces. Another viable strategy is to decrease the mobile phase flow rate to align with the plate height optimum linear velocity. However, this extends analysis time in proportion to the column length, limiting the utility of this approach. Increasing the column length is another potential option, but again it requires extended analysis time and increased pressure. An interesting solution to this problem emerged in the 1960′s [113]. This approach, known as recycling chromatography, operates on the principle of cyclical reintroduction of the sample zone into the column until its width equals one column length. By injecting a small sample volume, the process ends when a few compounds are fully separated. Under these conditions, the maximum allowable system pressure is no longer an issue, as only two columns are connected in series.

Recently, Gritti revisited recycling chromatography and noted the need to maintain a moderate pressure drop to limit the risk of column failure and pressure-dependent retention behavior [114]. This approach was successfully applied to an SEC separation of large molecules such as intact protein mixtures and mAbs. The employed apparatus was a straightforward twin-column recycling LC device [115]. The custom device was easily incorporated into standard HPLC or UHPLC instruments. This innovative strategy enabled the baseline separation and collection of two high-molecular-weight mAb aggregates from the main

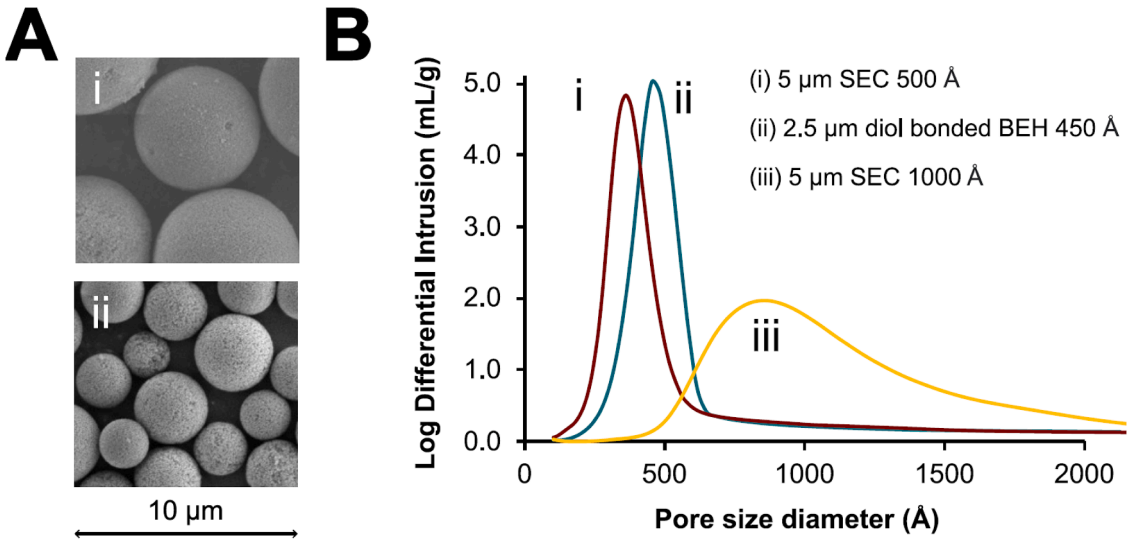

Fig. 9. A) SEM images of wide pore 5 µm silica 500 Å and (ii) 2.5 µm BEH SEC 450 Å Packing Materials. B) Mercury porosimetry can reveal pore size distribution for different packing material as indicated in the legend. Reproduced from [61].

mAb peak using two 150 mm long columns packed with 1.7 μm particles with a total of 8 cycles, leading to relatively long analysis times. Interestingly, in this example, the relative abundances of the two aggregates with respect to the monomer were 1:150 and 1:250, offering an additional level of complexity for their separation and UV detection.

More recently, this alternate pumping recycling SEC apparatus was found to be the most interesting technique to characterize mAb products and enhance the quantification of very low concentration fragment impurities. Fig. 10 shows the SEC analysis of a model 150 kDa mAb and the separation of its 100 kDa sub-units. When using a single column of 150 × 4.6 mm with 1.7 μm particles, the resolution between the mAb and the 100 kDa subunits was very low, making the accurate quantification of these impurities impossible. Some additional experiments were therefore carried out to simulate the use of very long columns. The number of cycles was increased from 1 to 10. The results indicate a significant improvement in resolution with an increasing number of cycles. The peak corresponding to the 100 kDa subunit was adequately separated after 3 cycles, and after 7 cycles, two distinct peaks were observed. Even if the analysis time increased with the number of cycles, it always remained below 1 hour (4 min longer per additional cycle).

In conclusion, despite the limited use of recycling LC, its potential in SEC is significant, which should lead to its broader adoption, both at the analytical and preparative scales. The development of commercial devices and suitable software for implementing such techniques for the analysis of biopharmaceutical products would be indeed highly advantageous.

4.5. Coupling SEC with MS

SEC separates molecules based on their hydrodynamic size, while MS provides information about molecular mass and structural details. Coupling SEC with MS provides a powerful analytical tool for the comprehensive characterization of complex biopharmaceutical products. It provides information about the distribution of molecular sizes within a sample and it can facilitate the determination of protein oligomeric states, post-translational modifications and identification of

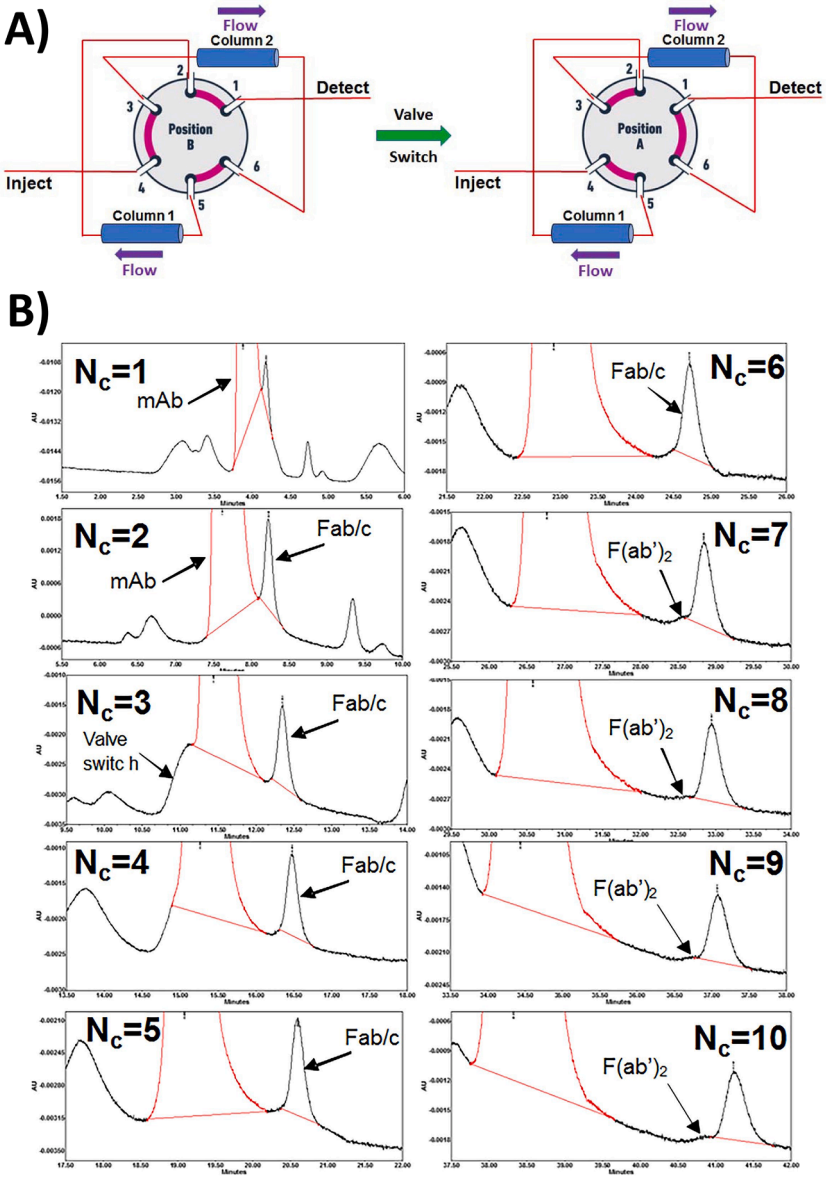

Fig. 10. Recycling SEC of a mAb. (A) Schematics and positions of the valve (two positions A and B, six ports 1–6) during alternate pumping recycling LC. (B) SEC experiments using two twin 4.6 × 150 mm 1.7 μm 200 Å BEH Columns for the analysis of mAb standard. The number of cycles was increased from 1 to 10. Adapted with permission from [204].

associated ligands or contaminants. However, SEC typically involves using aqueous buffers and mild conditions to maintain the native state of biomolecules, while MS often requires volatile solvents and acidic conditions for ionization. Achieving compatibility between these disparate conditions without compromising the integrity of the analytes can be challenging. Indeed, until 2015, the direct coupling of SEC to MS was rarely performed, primarily due to hardware limitations. Older MS instruments were unable to tolerate high salt concentrations, while SEC columns lacked the necessary inertness, resulting in generally suboptimal peak shapes, particularly when volatile salts were involved. Therefore, indirect coupling of SEC to MS was performed by the manual collection of SEC fractions that were analysed by direct infusion native MS (nMS), after tedious desalting protocols to switch to MS-compatible volatile buffers. A typical SEC mobile phase composition includes sodium or potassium chloride (generally between concentrations of 100 mM and 250 mM) and phosphate buffer salts in water (at a concentration between 50 mM and 200 mM). First attempts to direct coupling SEC to MS required the modification of SEC mobile phase from the standard phosphate buffer salts to MS compatible components, mainly consisting of ammonium acetate at concentrations between 25 mM and 100 mM [40]. In these early experiments, mobile phase flow rates were brought to relatively low linear velocities. For example, Heberger et al. [116] reduced the amount of salts entering the MS device by using a split to reduce the flow rate from 200 µL/min to 4 µL/min, before infusing the flow to the MS through a NanoMate™ direct infusion system. This strategy made it possible to accurately determine masses for size variants present in the sample, including both aggregates and impurities derived from the incorrect light and heavy chain association of a bispecific mAb [116]. In a feasibility assessment for future MS hyphenation, Goyon et al. [117] used an SEC column packed with sub-3 µm particles to characterize the profiles of 30 therapeutic mAbs and related products by comparing a standard SEC mobile phase (50 mM potassium phosphate buffer + 250 mM of potassium chloride) with an MS-compatible, 100 mM ammonium acetate mobile phase. Surprisingly, only five acidic therapeutic antibodies (with a pI < 7) could be successfully analyzed with the ammonium acetate mobile phase, as judged by obtaining peaks with tailing factor < 1.5 and baseline resolution (Rs > 1.5) between HMWS and the main chromatographic peak. Basic antibody products (pI > 7) required the use of a potassium-based mobile phase. This study highlighted the urgent need in obtaining even more inert stationary phases to maintain optimal SEC performance even when using MS-compatible mobile phases [117]. Despite this limitation, the coupling of SEC with MS found a second and very interesting purpose: a rapid and automated desalting of samples by eliminating tedious off-line buffer exchange protocols. An example of this approach was proposed by Ehkirch et al. for the analytical characterization of a variety of mAb-based molecules (i.e. mAbs, ADCs, bsAbs, and Fc-fusion proteins). In general, improved ESI efficiencies and enhanced signals were obtained at lower flow rates. Therefore, the first step of the study involved the optimization of the SEC flow rate to obtain the best balance between high MS signal intensity and efficient desalting. Decreasing the flow rate from 0.25 mL/min to 0.10 mL/min produced a 5-fold increase in MS peak intensities (Fig. 11A). Columns packed with 1.7 µm particles but having different nominal pore sizes and lengths were then evaluated. It was found that a 200 Å nominal pore size should be preferred in all cases. Longer columns (150 mm and 300 mm) were applied to reach best chromatographic efficiency and MS peak resolutions, while shorter columns (30 mm) made high throughput analysis possible. In comparison to the manual desalting process, online SEC desalting was significantly more effective, resulting in near baseline resolution of mAb glycoforms in the acquired mass spectra (Fig. 11B). A notable 6.7-fold increase in MS peak resolution was obtained for fast desalting compared to manual desalting when using the short 4.6 × 30 mm column. On the other hand, the best MS peak resolution was achieved with long 4.6 × 300 mm column, which yielded an 8-fold increase in MS peak resolution and improved mass accuracy. The possibility to use online SEC-nMS for more than online desalting was also evaluated through chromatographic analysis of a temperature-stressed NIST mAb (Fig. 11C). Both HMWS and LMWS peaks were simultaneously characterized by online MS data (Fig. 11D).

A detailed protocol on how to perform online SEC-based buffer exchange and nMS was also proposed by Wysocki et al. [118] The setup was tested on three MS instruments from different vendors and in each case the instrument was tuned to maximize desolvation and transmission of the ions of interest to demonstrate the suitability of the approach, regardless of the characteristics of the MS instrument.

To obtain optimal SEC-MS performance and keep the proteins in their native state when using volatile mobile phases, interactions between proteins and the column should be limited. For this purpose, Ventouri et al. [119]explored how the elution and ionization of proteins during SEC–MS analysis might be affected by volatile mobile phases. Using myoglobin as model protein the differences produced by use of different volatile salts (ammonium acetate, formate, and bicarbonate), ionic strength and pH were examined. Observing the charge state distribution of myoglobin and the loss of its heme component allowed estimation of potential interactions of myoglobin with the stationary phase during the SEC separation and denaturation that might occur during ionization. As previously discussed in section 2.5., it was found that volatile salts are effective but relatively high concentrations are needed to minimize secondary interactions. Also, when the mobile

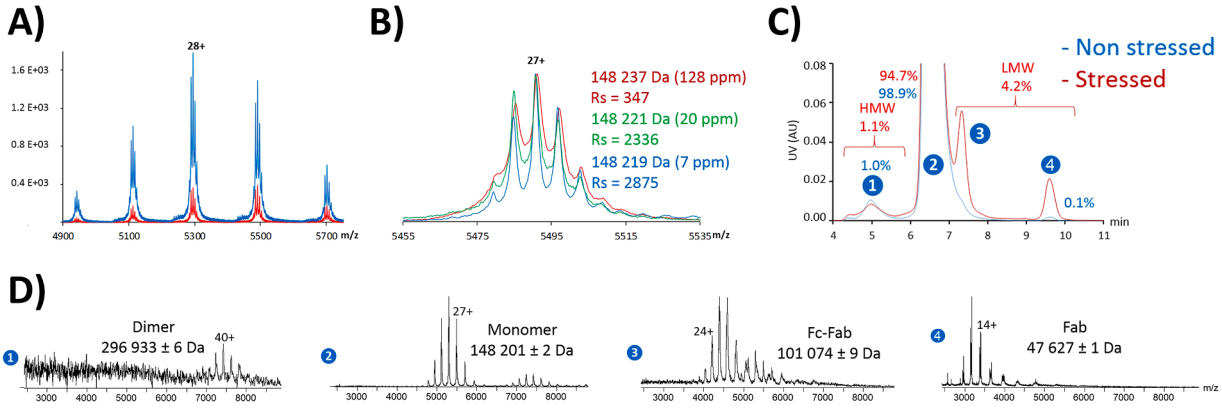

Fig. 11. Impact of flow rate and column dimensions on MS sensitivity and resolution (A-B) and online SEC-native MS analysis of temperature-stressed NISTmAb sample (C-D). A) Native mass spectra of trastuzumab analyzed by online SEC-native MS with a flow rate of 0.25 ml/min (red trace) and 0.1 mL/min (blue trace). B) Comparison of manual and SEC desalting efficiencies. Zoom on the 27+ charge state of trastuzumab manually desalted (red trace), analyzed by SEC-native MS with a 4.6 × 30 mm column (green trace) and a 4.6 × 300 mm column (blue trace). C) Overlaid SEC chromatograms of stressed (red trace) and unstressed (blue trace) NISTmAb. (D) Native mass spectra of each individual SEC separated peak for the stressed NISTmAb sample. Adapted with permission from [205].

phase concentration is too high, the protein analyte's interactions can be exacerbated. Conversely, lower ionic strength mobile phases failed to prevent electrostatic interactions between the protein and column material, resulting in significant protein adsorption and peak tailing in the chromatogram. These differences appeared to be primarily associated with the kosmotropic/chaotropic properties of the cationic salt additives. The elution profile's dependency on pH and ionic strength is heavily influenced by both the protein's physico-chemical characteristics and the material of the stationary phase. Consequently, these factors should be meticulously evaluated. Finally, formate, and particularly bicarbonate, [120] led to higher proportions of denatured protein species, while ammonium acetate demonstrated the most effective preservation of protein structure, especially when used at high ionic strength (200 mM) [119].

To limit possible unwanted interactions between proteins and the stationary phase and ensure optimal SEC-MS performance when using volatile mobile phases, innovative bioinert SEC columns have been proposed, as previously discussed. An interesting example is reported by Murisier et al. [121] that tested prototype metal-free SEC column hardware consisting of polyether ether ketone (PEEK) lined stainless steel tube including PEEK frits. The performance of this PEEK-lined column was systematically compared with conventional stainless steel SEC column hardware packed with the same stationary phase material for the analysis of different biopharmaceutical products (mAbs and ADCs). The mobile phase was comprised of 100 mM ammonium acetate. Significant differences were noted concerning the recovery of HMWS and the shape of monomer peaks. This confirms that chemical or adsorptive interactions do occur between the sample and metallic surfaces and that there is value to using metal free hardware. Furthermore, it was illustrated that the variations observed between the conventional and metal-free columns were pronounced, especially in the case of the most basic mAb products such as NISTmab, trastuzumab, and palivizumab (pI $>$ 9). This confirmed that electrostatic interactions might be accountable for this adsorption. Moreover, the successful utilization of the metal-free column enabled the execution of direct SEC-MS experiments on both regular and stressed/expired mAb products. Differences in the profile of size variants were identified between these two sample types, and the distinct peaks observed were readily discerned through the obtained mass spectra [121]. Another innovative low-adsorption SEC column was also tested by the same group [122]. This column consisted of metallic hardware components that were treated to have hydrophilically modified hybrid organic–inorganic silica surfaces, previously introduced in Section 3.2 as h-HST. The comparison between a reference stainless steel SEC column and the h-HST SEC column revealed improvements in band broadening, peak tailing, and HMWS recovery for complex mAb-related products. Evaluation of various mobile phases (such as phosphate and ammonium acetate with varying ionic strengths) identified 50 mM ammonium acetate as the optimal compromise between LC performance and MS sensitivity. Excellent repeatability in elution times and %HMWS was observed, although larger RSD values emerged between different UHPLC instruments, emphasizing the preference for low adsorption LC systems. Finally, optimized SEC conditions, combined with MS, facilitated the characterization of size variants in stressed and non stressed complex mAb products. This combination proved to be valuable in confirming proper dimerization and assembly of a bsAb therapeutic. These studies underscored the significance of both packing material chemistry and column hardware material in improving SEC-MS capabilities. Another strategy to improve ionization efficiency while preventing protein interactions with the stationary phase relies on using very high concentrations of volatile buffer (up to 400 mM) in combination with micro-flow SEC-nMS. In this context, Ventouri et al. [123] recently reported the use of narrow SEC columns (1.0 mm internal diameter) operated at 15 μL/min flow rate and coupled online to nMS for the characterization of proteins, labile protein complexes and low-abundant protein aggregates and impurities. Micro-flow SEC-nMS allowed the use of mild interfacing conditions (low desolvation flow and source temperature), interaction-free SEC, and an optimal detection of low-abundance protein species. This strategy is a valuable option for applications with limited sample availability.

4.6. Coupling SEC with new detectors

Biopharmaceutical products are evolving at a rapid pace and new modalities including mAb-related compounds, gene therapy, and mRNA products have already been approved and made available for the treatment of various pathologies. What unites these new modalities is their structural complexity and especially their large size, ranging from the kilodalton (kDa) range in the case of mAb-related compounds to the megadalton (MDa) range for viruses applied as vectors in gene therapy. As previously discussed in Sections 2.7 and 3.5, SEC-MALS and SEC-MS can be successfully applied for the size characterization of these biopharmaceutical products, although alternative detectors and techniques for high mass measurements are emerging and might be classified based on the size of the analyte that they are able to analyze. In this context, mass photometry (MP), originally introduced as interferometric scattering mass spectrometry (iSCAMS), is generally able to detect analyte in the range of 30 kDa – 6 MDa [124]. Charge detection MS (CDMS) has been applied for analytes up to 10 MDa, [125] while gas-phase electrophoretic mobility molecular analyzer (GEMMA) and nano-electromechanical system-mass spectrometry (NEMS-MS) have been applied for analytes of $\sim$ 25 MDa and $\sim$ 100 MDa, respectively [126–128]. However, direct coupling of SEC to these alternative detectors has only been reported for MP and CDMS. These two techniques will be discussed in more detail.

Mass photometry (MP) is a technique used to measure the mass of individual biomolecules in solution by analyzing their light-scattering properties with interferometric scattering microscopy. It operates on the principle that as molecules pass through a focused laser beam, they create disturbances in the beam due to the way they interact with light. Once the light scattering of biomolecules is detected, it can be directly used to extract the molecular mass [129]. On the other hand, charge detection mass spectrometry (CDMS) is a single-particle technique able to simultaneously measure the charge (z) and mass-to-charge ratio (m/z) of individual ions and thereby directly determine molecular weight information without the need to deconvolute charge state distributions [129]. Both techniques might be particularly effective for studying large molecules like proteins, nucleic acids, nanoparticles, and viral vectors, providing insights into their mass and concentration [125,129,138–140, 130–137]. In this context, Heck et al. reported an interesting comparative analysis of heavily glycosylated macromolecular immune complexes by SEC-MALS, nMS, MP, and CDMS [141]. Highly heterogeneous immune activation complexes, constituted by the sEGFR (soluble domain of the epidermal growth factor receptor) antigen bound to the IgG1 mAb hexamer initiated by complex C1q, were evaluated. As reported in Fig. 12, the final $(sEGFR)_{12}$:$(IgG1)_6$):C1q immune complex was confidently assigned with MP and CDMS, overcoming certain limitations in the mass measurements encountered with conventional nMS (inability to resolve charge states prevented mass determination) and SEC-MALS (insufficient mass accuracy for determining exact stoichiometries). However, it is worth mentioning that MP, nMS, and SEC-MALS performed well in the analysis of immune complexes of smaller size prior to the addition of sEGFR antigen (top panels of Fig. 12A-C). As discussed by the authors, SEC-MALS is accurate for small proteins, but it could underestimate the masses of larger constructs or multicomponent systems as much as 10 – 20%. This is why alternative detectors such as MP and CDMS could be valuable alternatives. SEC-MP was applied to the analysis of an AAV drug product. AAV monomers were separated from impurities by SEC, while the fraction of fully packaged AAVs in the total population of AAV particles was estimated by MP [142]. SEC-MP coupling was performed offline by collecting SEC fractions that were diluted at a proper concentration (10^{11} particles/mL)

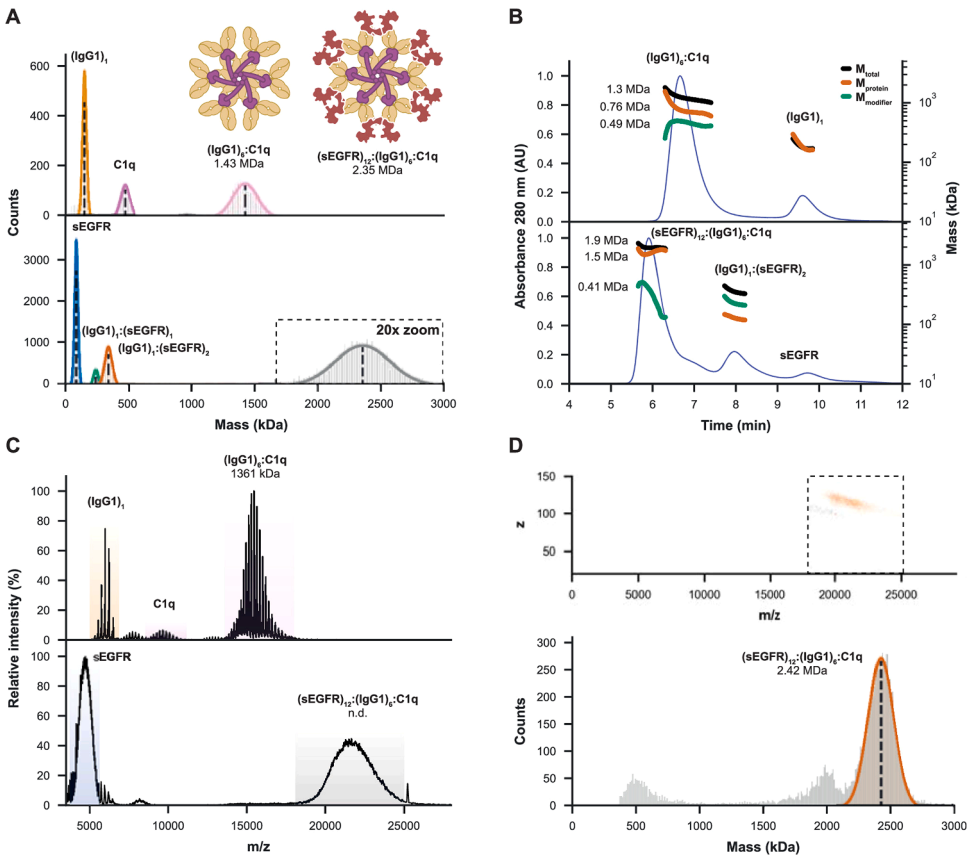

Fig. 12. Comparative analysis of highly heterogeneous immune complexes by MP (A), SEC-MALS (B), nMS (C), and CDMS (D). (A) MP measurements of the complex (top). (B) SEC-MALS-UV-RI analysis similarly reveals the formation of ~1.3 MDa complex (top). When sEGFR was added (bottom), SEC-MALS-UV-RI revealed the formation of larger complexes of around 1.9 MDa. (C) Measurement of the same samples by native MS reveals an accurate mass (top), but the technique struggles with complexes involving sEGFR (bottom). (D) Single-particle measurements of the distribution around *m/z* 21,000 by CD-MS (top) revealed a mass of 2.42 MDa (bottom) corresponding to the expected mass of the full sEGFR complex (bottom). Adapted with permission from [141].

[143] prior to loading the MP coverslip. The SEC mobile phase consisted of phosphate buffer at pH 7.4 with 350 mM NaCl and MP settings were optimized for the analysis of AAVs in the range from 3 MDa to 6 MDa. Fully packaged AAVs could thus be distinguished in heterogeneous samples in order to more accurately determine a potency correlated titer.

In other labs, SEC has been directly coupled with CDMS for the characterization of synthetic polymer of ultra-high mass (5–6 MDa) [144] and different proteins, including a mAb and a highly glycosylated Fc-fusion protein [145]. In this latter case, the SEC mobile phase consisted of 100 mM ammonium acetate flowing at 50 µL/min. Column effluent was directly interfaced to the CDMS. A mixture of two complex glycoproteins, namely AGP (α−1-acid glycoprotein) and the Fc-fusion protein etanercept, was used as an example sample. Both of these glycoproteins contain numerous glycosylation sites, so they both exhibit broad and complicated mass distributions [145]. By using the SEC-CDMS approach, these two glycoproteins were chromatographically separated and their predominant masses were measured, allowing a quick assessment of their overall microheterogeneity.

4.7. Multidimensional chromatography with SEC

SEC has been widely used in two-dimensional liquid chromatography (2D-LC), as both a first (^{1}D) and second (^{2}D) dimension. It has even been used in multidimensional (mD-LC) setups for the fast and effective characterization of different biopharmaceutical products. The first attempts at this were with heart-cutting 2D-LC, where Protein A affinity chromatography was used in the ^{1}D, and SEC was used in the ^{2}D for the characterization of mAb samples [146,147]. In one case, Sandra et al. presented examples related to trastuzumab and tocilizumab biosimilar development programs. Different mAb producing CHO clones were analysed in comparison to their originator and the 2D Protein A-SEC setup was able to guide clone selection based on titer and product purity. The Protein A mobile phase was adapted to avoid UV disturbances in the ^{2}D. Use of acetic acid instead of citric acid was advantageous. However, this setup was not directly compatible with MS detection as SEC in the ^{2}D was performed by using non-volatile mobile phase components. Another interesting 2D-LC setup including SEC in the ^{2}D was proposed by An et al. for the study of forced degraded mAbs with a multiple heart-cutting IEX-SEC 2D-LC setup [148]. This interface consisted of one 2-position/4-port duo valve in combination with two 6-position/14-port valves. Twelve fractions could thereby be collected. The charge variant peaks in ^{1}D IEX were collected and analysed in the ^{2}D SEC. Like the previous case, this setup was not directly hyphenated with MS detection as the SEC was performed with non-volatile mobile phase [148]. More recently Lambiase et al. reported the reverse setup consisting of a heart-cutting SEC-CEX 2D-LC workflow [149]. In this case, SEC was placed in the ^{1}D for aggregate quantification, followed by online fraction transfer of the monomer peak to the ^{2}D for charge variant analysis by CEX. In addition, this SEC-CEX separation was developed with volatile mobile phases (consisting of 200 mM ammonium acetate for SEC and the Waters IonHance™ CX-MS Buffers for CEX). Direct hyphenation to MS and online charge variant peak identification was achieved. SEC in ^{1}D was also used in a 2D-LC (SEC-HIC) and a 4D-LC-MS (SEC-reduction-digestion-RPLC-MS) setup developed by Goyon et al for the characterization of ADC products, where the goal was to investigate the role of drug-to-antibody ratio (DAR) species on aggregate formation [150]. First, the monomeric ADC species were separated from the

aggregates by SEC in the ^{1}D under non-denaturing conditions (100 mM potassium phosphate and 200 mM potassium chloride in 95:5 water: propanol). The SEC column effluent was then mixed with the HIC mobile phase A (1.5 M ammonium sulphate in 25 mM potassium phosphate in 80:20 water:propanol) at 1:3 ratio before collection and storage of fractions prior to their analysis by ^{2}D HIC. To retain proteins on a HIC stationary phase, high concentrations (> 1 M) of strongly kosmotropic salts, such as ammonium sulfate, are required. This adsorption was not achieved with the SEC mobile phase. To achieve facilitate adsorption to the HIC column, flow from the ^{1}D SEC column was merged with the HIC mobile phase A during the collection of the SEC fractions. Then, the 2D-LC (SEC-HIC) technique was applied to compare the average DAR values of the main peak species and the aggregates. The same ^{1}D SEC was then used in the frame of a 4D-LC-MS setup to determine the levels of potential critical quality attributes (CQAs) including aggregation, average DAR, oxidation, and deamidation. The 4D-LC-MS workflow consisted of SEC in the ^{1}D (operated in the same conditions as previously described but without the premix of the mobile phases during fraction collection), then on column reduction and subunit analysis in ^{2}D, tryptic digestion in a flow-through mode in the ^{3}D, and peptide mapping in the ^{4}D with hyphenation to MS detection. In this case, only the ^{1}D and ^{4}D were separative dimensions. The ^{2}D and ^{3}D were automated sample preparation steps. Finally, three different size variants, namely, the main peak, dimeric species, and higher-order aggregates, were simultaneously separated, fractionated, and analyzed by reduced RPLC followed by on-line peptide mapping allowing the analysis of additional CQAs such as oxidation and deamidation. Interestingly, the use of SEC in the ^{2}D or ^{3}D of a mD-LC-MS setups was also applied to perform an automated desalting step of the mobile phases used in the ^{1}D so that native MS (nMS) analysis could be quickly performed [151–154]. This strategy was first applied by Ehkirch et al. in a comprehensive 2D HICxSEC setup coupled to ion mobility (IM) and MS detection (HICx-SEC-IM-MS) for the characterization of an interchain cysteine-linked ADC (brentuximab vedotin) [151]. For this purpose, non-volatile HIC mobile phases were used for the first dimension, while 100 mM ammonium acetate was used for the second dimension. In the ^{1}D, the average DAR and the drug load distribution (DLD) profile of the ADC was evaluated. Then, the salts employed in HIC were eliminated by a size-based separation in the ^{2}D SEC. Indeed, in this configuration, SEC was not intended for separating ADC aggregates but exclusively used as fast desalting step. In addition, by using an external two-position switching valve, the fraction with no salts was sent to the MS, while the fraction containing the salts was diverted to the waste to avoid contamination of the mass spectrometer. With this setup, each HIC peak separated in the ^{1}D was MS identified and structurally characterized by IM-MS. By using the same setup (2D-LC-IM-MS), the authors also explored comprehensive 2D SECxSEC analysis to run SEC with non-volatile salts in the ^{1}D followed by automated desalting by SEC in the ^{2}D [152]. In this case, a non-volatile SEC mobile phase (50 mM of phosphate buffer and 250 mM potassium chloride) was used in ^{1}D, 100 mM ammonium acetate was used in ^{2}D, and the same external switching valve of the previous setup was kept to divert the fractions containing the salts to the waste before the introduction of the flow to the IM-MS instrument. The SECxSEC-IM-MS setup was applied for simultaneous detection, identification, and quantitation of adalimumab size variants and forced degraded pembrolizumab and bevacizumab samples. It was crucial for the assessment of unexpected high/low molecular weight species. Going in the same direction, Verscheure et al. reported a 3D-LC-MS setup consisting of Protein A affinity chromatography in the ^{1}D, a multidimensional option in the ^{2}D, and SEC in the ^{3}D [153]. This 3D-LC-MS setup was configured with an automated ^{2}D mode switching offering the opportunity to choose between three different chromatographic modes (SEC, CEX, and HIC) by the incorporation of a column selector valve. To allow the switching among different ^{2}D modes, the system was preconditioned by flushing with the mobile phase composition of the desired chromatographic mode followed by a blank run to fully condition the column before sample injection. The authors proved that it was possible to run the three different ^{2}D modes in one sequence without losing chromatographic quality. Therefore, this innovative 3D-LC-MS setup was able to perform the simultaneous and sequential assessment of mAb titer, size/charge/hydrophobic variants, MS based evaluation of the molecular weight, and the characterization of post-translational modifications (PTMs) directly from cell culture supernatants. The methodology was successfully applied to the analysis of trastuzumab and tocilizumab originators and different mAb-producing CHO clones.

4.8. Innovations in preparative SEC of proteins

SEC has been widely applied for analytical separations of proteins. However, its utility at the preparative scale has been limited due to inherent drawbacks such as low speed, limited loading capacity and scalability [155]. Increasing the length to particle size (L/d_p) ratio can increase resolution at the analytical scale, but this strategy is less interesting during scale-up, particularly when soft chromatographic media, prone to resin compaction and non-uniform column packing, are employed [156,157]. To address these limitations, a flat cuboid chromatography device named z^2 cuboid SEC device has been introduced. This device improves the use of the SEC medium volume by optimizing column shape, length, and internal diameter. The z^2 cuboid SEC device is characterized by a short and wide column which efficiently limits macroscale convective dispersion, thanks to its flow distribution and collection features [158]. While designing this device, the z^2 researchers systematically compared the resolution achieved with a short and wide SEC column (60 × 22.6 mm) versus a conventional SEC column (300 × 10 mm), both packed with Sephacryl™ S-200 HR material and having a total volume of 24 mL [158]. Model proteins, BSA and lysozyme, were used to evaluate the performance of the new device. The obtained results demonstrated that the short and wide column exhibited poorer separation in SEC compared to the taller column with an equivalent volume, mostly due to the adverse effects of macroscale convective dispersion [159–161]. Subsequently, the authors evaluated the z^2 cuboid SEC device with a volume of 24 mL (cross-sectional dimensions of 20 × 20 mm and height of 60 mm) and compared the performance with a conventional 300 × 10 mm SEC column. Notably, the BSA and lysozyme peaks obtained with the z^2 cuboid SEC device were narrower (30% better resolution) without signs of fronting or tailing, and the loading capacity was enhanced.

The study further explored scalability by increasing the z^2 cuboid SEC device volume from 24 to 200 mL (cross-sectional dimensions of 40 × 40 mm and height of 125 mm). Excellent resolution was achieved with the enlarged z^2 cuboid SEC device, even at very high flow rates (up to 20 mL/min) and with concentrated protein solutions (40 mL injection of a solution containing 10 g/L BSA and 4 g/L lysozyme). The total run time was reduced to 25 min, which would normally require more than 100 min for a similar conventional separation.

These findings highlight the potential of the z^2 cuboid SEC device as a valuable approach to enhance speed, loading capacity, resolution, and scalability of preparative SEC. This should contribute to the broader adoption of SEC as a mainstream protein biopharmaceutical purification tool. Nevertheless, future investigations should validate this strategy on more relevant samples, such as mAb drug substances containing LMWS and HMWS.

5. Applications of SEC

Table 3 provides a summary of recent representative applications of SEC in analysis of protein biopharmaceuticals and emerging gene therapy products. These diverse examples are further discussed below.

Table 3
Summary of recent representative applications of SEC in analysis of protein biopharmaceuticals and emerging gene therapy products.

Modality	Application	Detection	References
ADC	Drug to antibody ratio, drug load distribution, free drug/ antibody level quantification	MS	[79,178,179]
bsAbs	Size variant and chain association analysis	MS	[122,181,182]
Plasmid DNA	Isoforms quantification	UV	[22,64,188]
mRNA	Poly(A) analysis, HMWS and heterogeneity analysis	UV	[22,64,193]
mRNA/LNPs	Size and heterogeneity analysis	UV, MALS	[22,63,97]
AAVs	Capsid, genome and HMWS quantification, empty/full ratio determination	UV, MALS, FLR, mass photometry	[61,62,94, 142,194,195, 196,197]
Other viral and viral-like vectors	Quantification, size variant analysis	UV	[70,198,199]

5.1. Protein biopharmaceuticals

SEC is routinely used in QC and development laboratories to achieve the separation and quantification of HMWS and LMWS. These molecular weight species are of particular concern to health authorities because of their potential impact on safety, potency, and pharmacokinetics of drug products. Recommended SEC operating conditions for the analysis of recombinant mAbs have been published in the U.S. Pharmacopeia (USP) General Chapter ⟨129⟩ and by several international regulatory organizations [162–164]. To meet regulatory expectations, biopharmaceutical companies need to demonstrate the suitability of their SEC methods in terms of specificity, linearity, accuracy, precision, robustness, and detection and quantification limits [165–169]. General SEC applications, which have also been partly discussed in the previous paragraphs, include the use of SEC during mAb development processes and manufacturing control, [166,170,171] such as the guided selection of a cell line capable of producing low levels of aggregates, the optimization of the purification steps by monitoring the levels of high molecular weight species, and the precise quantitation of aggregates during formulation development [153,154,172–174]. However, it should be noted that complex protein biopharmaceuticals such as ADCs, bi- and tri-specific antibodies (bsAbs), or Fc-fusion proteins can be more challenging than the typical two-light-chain/two-heavy-chain mAb products. As such, classical SEC methods may not be suitable for these samples [175,176]. In this section, a particular emphasis was therefore dedicated to the applications of SEC for the analysis of these more complex, mAb-based biopharmaceutical products.

ADCs are a clear example of enhanced mAb structural complexity. The composition of a linker-payload conjugated mAb must be tested for the usual CQAs of antibody products. Yet, they also need to be tested for average drug to antibody ratio (DAR), drug load distribution (DLD), and level of free drug and free antibody. Conjugated cytotoxic payloads are often very lipophilic and their simultaneous analysis with other product attributes can help improve the throughput of an analytical technique. In this context, Goyon et al. investigated the role of SEC analysis in the evaluation of the level of free drug (here a lipophilic payload) while also performing a size-variant separation of an ADC [79]. Size-variants were first separated by an SEC column packed with 2.0 µm particles and

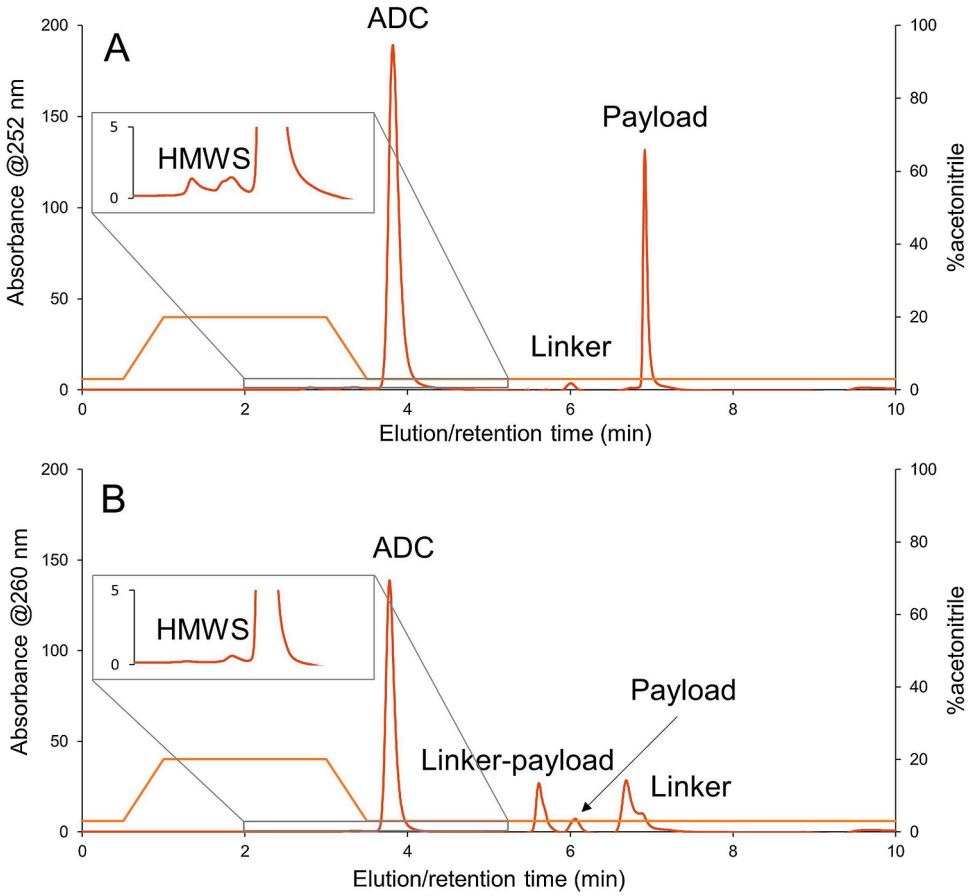

Fig. 13. Separation of free payloads, linkers and linker-payloads by a generic gradient SEC method for ADC1 (A) and ADC4 (B). Gradient conditions = Mobile phase B composition (acetonitrile) was increased from 0.5 to 1.0 min from 3% to 20% to elute the hydrophobic species, then kept at 20% for 2 min, and then decreased from 20% to 3% in 0.5 min to finally equilibrate the column from 3.5 min to 10 min. Adapted with permission from [79].

mobile phase conditions of > 0.3 M potassium-based salts in water. However, the analysis of the free payload alone under the same isocratic conditions demonstrated that secondary hydrophobic interactions hampered the elution of the free payload unless 20% organic modifier was added to the mobile phase. Therefore, to obtain the simultaneous characterization of the more lipophilic free payload together with the size-variants, gradient elution was evaluated by using mobile phase A consisting of 0.05 M potassium phosphate buffer + 0.25 M potassium chloride in water at pH 6.8, together with mobile phase B composed of pure acetonitrile (Fig. 13). These conditions allowed the researchers to obtain the separation of the size-variants within the column dead time (6.5 min) plus the elution of the linker, payload, and linker-payload, based on their increasing lipophilicity with an RPLC-based separation across the SEC column. In addition, aggregate levels were found to be consistent between the analysis performed with the gradient SEC method and the amounts of HMWS obtained when using a purely aqueous mobile phase, proving that native conditions were maintained when using the gradient SEC method.

In a more recent contribution, Thomas et al. developed an automated 2D SEC-RPLC-MS workflow to characterize ADCs and specifically the small molecule drug while conjugated to the mAb [177]. In this approach, the ADC deconjugation was obtained by an autosampler using a defined program and the ^{1}D SEC was used to achieve the separation between the small molecule and protein species. Then, the small molecules were trapped and sent to the ^{2}D RPLC for separation and quantification, with additional MS identification of impurities and degradants. As the ^{1}D SEC was not directly connected to the MS, canonical mobile phase conditions were applied, although an organic modifier was added to the composition. The automated method was assessed in terms of specificity, sensitivity, linearity, and precision, and proved to be stability indicating for a model ADC.

Following the ICH guideline Q2(R1) on validation and analytical procedures, [164] Jones et al. assessed the potential of SEC-nMS as a quantitative DAR method for the analysis of interchain cysteine-linked ADCs with DARs ranging from 2 to 8 [178]. Hydrophobic interaction chromatography (HIC) and SEC-nMS were employed to test these molecules, and the obtained DARs from both techniques were compared to evaluate the alignment of SEC-nMS quantitation with the HIC release assay. In this case, a microbore SEC column was used to desalt the ADC into ammonium acetate and facilitate online native MS analysis. Results suggested that SEC-nMS quantitation of a DAR does not introduce bias, and SEC-MS data can be correlated with HIC data without requiring a correction factor. Additionally, SEC-nMS was determined to be suitable for unbiased DAR quantitation in other ADC chemotypes. In summary, the study supported the conclusion that SEC-nMS is well-suited to accurately quantifying DAR in various interchain cysteine-linked ADCs.

SEC-nMS (among others LC-MS approaches) was also applied by Deslignière et al. to the characterization of trastuzumab deruxtecan (T-DXd), a third generation Cys-linked ADC, which is highly homogeneous with a DAR equal to 8 [179]. The use of a bioinert SEC column allowed the analysts provided a reliable separation and quantification of both HMWS and LMWS with a 50 mM ammonium acetate mobile phase. As shown in Fig. 14, this SEC-nMS analysis confirmed the presence of monomeric T-DXd glycoforms, low amounts of dimers (~5%), and very low levels of any LMWS (<1%). 8 and 16 drugs were attributed to the monomer and the dimer, respectively. In addition, after enzymatic *IdeS* digestion, the ADC subunit analysis by SEC-nMS enabled a more precise overview of the localization of the drugs on the Fab subunit, while confirming the glycan profile on the Fc portion.

Bispecific antibodies (bsAbs) and related products are another clear example of enhanced mAb structural complexity as they might be constituted by more than 100 different combinations of antigen-binding moieties and (homo/hetero) dimerization modules [180]. As bsAbs can be constituted from different domains, the proper chain-association is one of the most critical analytical challenges to monitor during bsAbs development and production. It is worth reviewing a couple examples of SEC-nMS being applied to the analysis of bsAbs. Duivelshof et al. have used the technique to characterize the size variants and proper chain-association emicizumab, [181] a bsAb having 1 + 1 asymmetric format with heterodimerizing heavy chains and common light chains. Meanwhile, Murisier et al. [122] investigated the size variants of 3 non-commercial bsAbs, consisting of a mAb bearing an additional

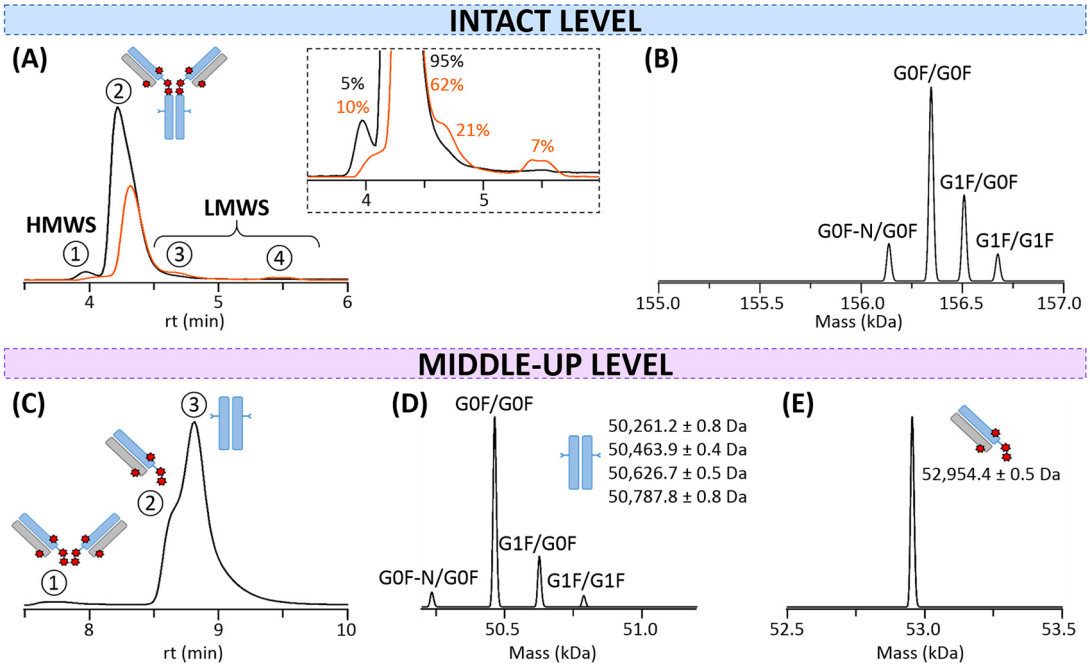

Fig. 14. SEC-nMS analysis of the ADC trastuzumab deruxtecan (T-DXd). (A) SEC-UV chromatograms of intact (black) and thermally-stressed (orange) T-DXd. Inset: Focus on minor species and their corresponding relative amounts. (B) Mass deconvolution of the intact monomer (peak 2) for the non-stressed sample. (C) SEC-UV chromatogram of *IdeS*-digested non-stressed T-DXd. (D) Mass deconvolution of the Fc subunit. (E) Mass deconvolution of the Fab region. Adapted with permission from [179].

N-terminal domain (~200 kDa), a mAb bearing a cytokine, and an additional domain in C-terminal position (~165 kDa and ~200 kDa, respectively). In both contributions, low adsorption SEC columns were used in combination with MS-compatible ammonium acetate mobile phases, and HMWS consisting of dimeric species were baseline separated from the monomeric bsAbs. In this case, coupling SEC to MS was essential for the identification of each species and to exclude the presence of side-products having an incorrect chain configuration. Another interesting example concerning the SEC-nMS characterization of high-molecular weight by-products in the production of a trivalent bispecific 2 + 1 heterodimeric antibody was reported by Cramer et al. [182] Here, the separation of the highly heterogeneous HMWS was essential to obtaining a detailed MS analysis of the by-products, mainly consisting of tetravalent variants. In addition, the characterization was linked to functional assays, changes in potency amongst of the variants, and altered biological activities.

Finally, it should be mentioned that cutting edge SEC techniques are making it possible to investigate multiple CQAs with a single apparatus. New instrument and experimental considerations are also helping analysts achieve multi-attribute measurements. In this context, beyond the examples already discussed in Section 3.7, we should point out an interesting universal eluent system proposed by Schwahn et al. [183] As shown in Fig. 15, the four lines of a quaternary pump were set up to deliver ultrapure water (line A), 1 M NaCl stock solution (line B), and undiluted 10X CX-1 pH buffer concentrate pH 5.6 and pH 10.2 in lines C and D, respectively. The modulation of the percentages of each line made it possible to tune a mobile phase composition for multiple types of chromatography. In fact, the approach facilitated the quick development of ion exchange techniques in addition to HIC and SEC. Automatic pH screening for a given separation mode was configured along with automated column selection. For example, SEC was performed on a mAb with 150 mM NaCl, after a 15% mixing of the 1 M NaCl solution in line B was selected and the mobile phase pH was set to 6.5 using 8% of line C and 2% of line D.

SEC is generally not considered a high throughput technique. However, recent advancements in multidimensional LC configurations and SEC column hardware are challenging this perception.

5.2. Gene therapy products

Gene therapeutics are complex medicinal products that require careful characterization to ensure their safety and efficacy. SEC, as a high-throughput and multi-CQA providing technique, is predicted to play an increasingly important role as an analytical tool to ensure quality and hasten the development of new products [184,185]. As introduced in Section 3.3, many of these new modalities are large molecules that require SEC columns with increasingly larger pore sizes. Historically, such wide pore SEC columns (up to 2000 Å) were successfully used for the purification of various forms of RNA, [186] and more recently also circular RNA [187].

SEC applications for nucleic acids on the analytical scale has been less common, possibly due to its relatively low resolution, and some related limitations on investigating the heterogeneity and integrity of an mRNA drug substance. To a certain extent, this issue is exacerbated by the prevalent use of columns with sub-optimal pore size (300 Å) [188]. Recent USP guidelines for mRNA vaccines development, recommend more appropriate columns (1000 Å) [189]. Interestingly, other voices in both industry and academia have not yet envisaged the use of SEC for the measurement of CQAs of RNA products [189–191]. This oversight might be due from a limited availability of columns that are suitably designed for this purpose. Historically, advancements in SEC column technology over the past twenty years have been driven by a deepening understanding of protein characteristics and behaviors. A similar effort is now required to extend these technological and methodological advancements to the analysis and study of nucleic acids.

Nucleic acid SEC is now a rapidly evolving topic. This can be seen with a recent study involving the use of prototype 3 µm SEC columns with a nominal pore size of around 1300 Å. These columns and corresponding methods were demonstrated to be useful for the i) discrimination of different plasmid DNA topological forms and the ii) comparison of mRNA drug substance materials and their aggregates [22]. SEC-UV profiles revealed differences in the quality of commercially available eGFP mRNA samples and differing levels of aggregates that could be removed by heat treatment (Fig. 16A). In an even more striking example of resolving power, these wide pore SEC columns produced a separation of open-circular and supercoiled pDNA species (Fig. 16B). An SEC separation such as this was confirmed to be

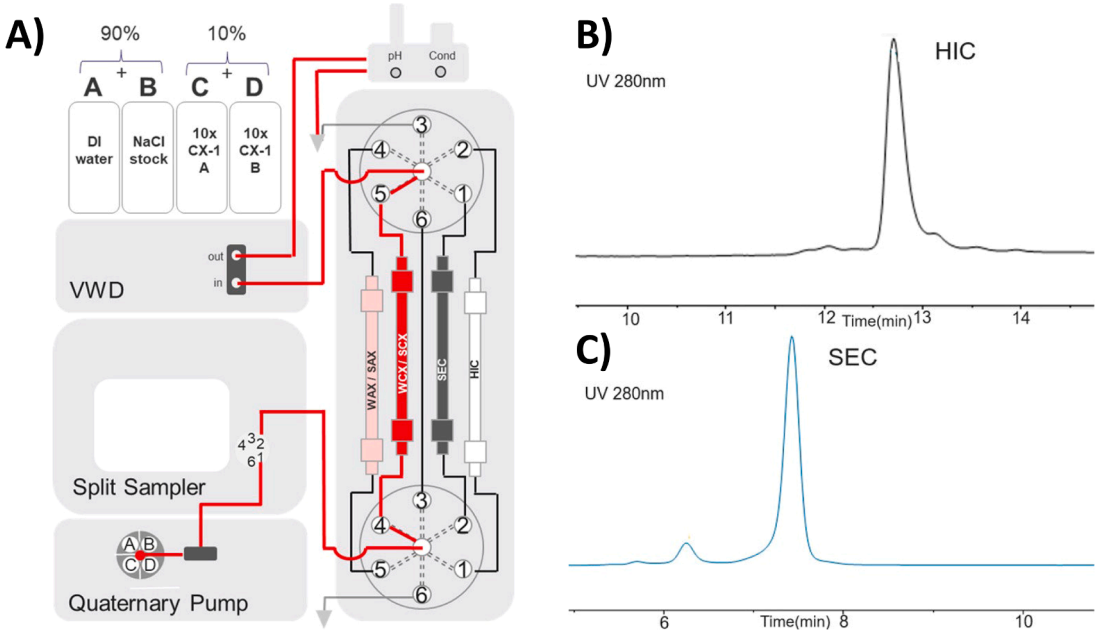

Fig. 15. Simplified flow diagram for the universal eluent system (A). Application of the universal eluent system applied to hydrophobic interaction chromatography with rituximab (B) and size exclusion chromatography with a proprietary mAb (C). Adapted with permission from [183].

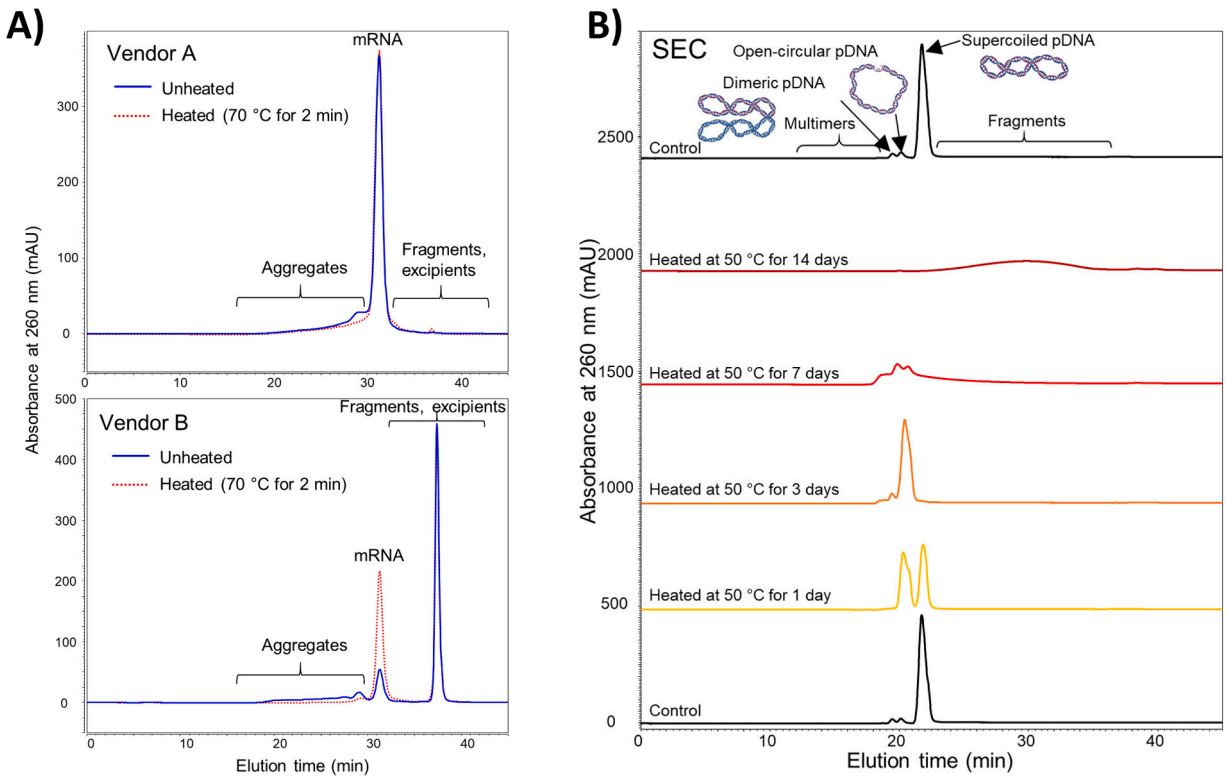

Fig. 16. SEC separation of various gene therapy products on prototype 1300 Å columns. A) Study of aggregates found in commercial eGFP mRNA samples. B) Analysis of pDNA topological forms in a thermal stress experiment. Reproduced from [22] with permission.

complementary to a commonly used AEX technique, though the SEC separations showed an additional benefit of better analyte recovery.

Apart from the analysis of intact species, SEC can also be used for orthogonal determination of specific CQAs of mRNA molecules. Gilar et al. used 250 Å pore size columns for the characterization of a cleaved RNA poly-adenine (poly(A)) tail to obtain information on its length and heterogeneity [64]. They showed that reliable results are possible for oligonucleotides up to 150 nt using dA_n calibration standards and an appropriately constructed calibration curve. However, the technique provided poor resolution between larger n, $n+1$ oligonucleotides than an ion pairing reversed phase separation, and only average length could be determined.

Another area of interest is the characterization of the LNP drug products. Historically, few stationary phases could be applied to similar modalities – liposomes. Mostly, size exclusions had been applied for purification purposes, because of strong interfering secondary interactions [192]. In fact, in one of the few reported SEC analyses of LNPs, it was actually a positively charged surface stationary phase that was applied [63]. This introduced a repulsive effect between the studied LNPs and the packing material, such that an online determination of RNA content in the LNPs could be performed (Fig. 17) [193]. When it comes to comprehensive sample analysis, caution should be applied with this approach, as it might not be suitable for nucleic acid analysis, due to the risk of adsorption and incomplete elution of negatively charged mRNA impurities.

The emergence of new low adsorption, high efficiency SEC columns holds great promise for this field. A recent report has shown that an SEC column packed with a neutral, hydrophilic packing material can be used to for MALS characterization of Fab conjugated LNPs [22]. Further literature showcasing applications of SEC to this type of modalities are needed [189].

One of the more advanced applications of SEC in the field of gene therapeutics is the analysis of adeno-associated viruses (AAVs), which are used as carriers of genetic material for 5 currently approved gene therapies. There are many additional AAV gene therapies in the pharmaceutical pipeline, which underscores the significance of developing

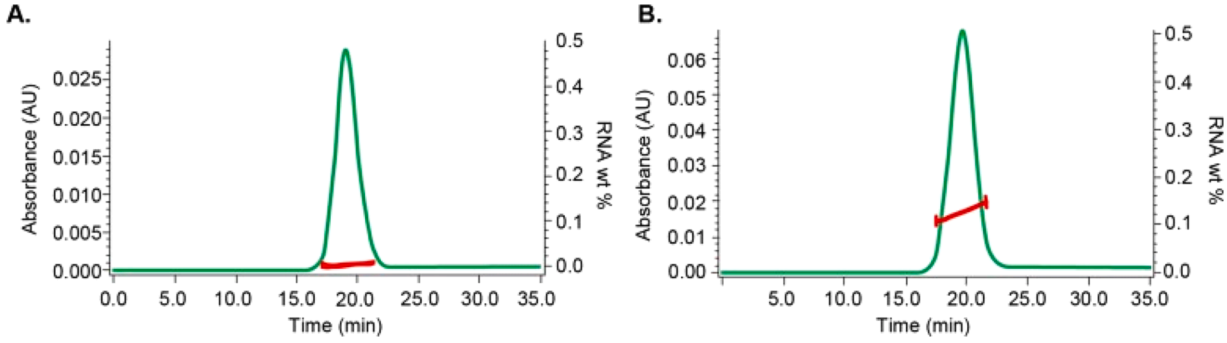

Fig. 17. SEC analysis showing 260 nm absorption profile and MALS determined RNA content for A) empty LNP B) full LNP sample. Reproduced from [193] with permission.

new analytical techniques for their characterization and release testing [185]. These spherical, approximately 25 nm particles can be comprehensively analyzed with SEC coupled to various detectors [194]. Even with basic UV detection, an SEC separation can provide measurements on several key CQAs such as titer, empty/full particle ratio and aggregate level. Quantification is best performed with fluorescence detection, which was reported to be 2–3 times sensitive than UV [195]. On the other hand, detection of multiple UV wavelength allows precise estimation of the capsid filling ratio [62]. A detailed study on aggregation has shown the suitability of efficient 2.5 μm 450 Å and 3 μm 700 Å columns for fast assessment of HMWS, despite elevated pressures. Robust and reproducible aggregate quantification was achieved with a platform method amenable to the analysis of several serotypes (Fig. 18) [61,196].

The utility of SEC is even greater when coupled to MALS - as it was shown to be a valuable, easily applicable tool for developability studies in a AAV-based preclinical stage program. SEC-MALS can reduce the analytical workload with its multi-attribute CQA measurements, that do not require calibration curves [94,197]. Similarly, coupling SEC to the output of a mass photometer allows orthogonal measurements of capsid filling with a noteworthy ability to estimate partially filled particles [142].

SEC has also been applied to the analysis of other viruses and viral like particles, more commonly used in vaccines [70,198,199]. Other viral vectors that are used in gene therapy are usually larger (which permits delivery of larger genes) like adenovirus (70 – 90 nm, Ad), lentivirus (80 – 120 nm, Lv) or herpes simplex virus (>160 nm, HSV) [200]. Accordingly, their analysis will require even wider pore columns. Despite its potential, examples describing applications of SEC to such analytes are scarce, and further work with suitable columns is needed to ensure the validity of the technique.

6. Conclusion

As demonstrated in this review, there have been some significant improvements in SEC over the last few years, both in terms of technology and application areas. The increasing interest in SEC is obviously related to the need to characterize more and more complex biopharmaceutical products. Nevertheless, SEC method development remains quite straightforward, as it is only a filtering technique. Indeed, this type of chromatography does not require extensive knowledge of the physicochemical properties of the analyzed molecules for successful method development. Consequently, its application has been thriving in recent years, most especially for the analysis of mAbs and related compounds, gene therapy products and mRNA samples. Currently, an important trend in SEC is the need to develop platform methods that enable analyses of a wide range of molecules of the same nature.

When conducting modern SEC, it is essential to preferentially select a low-adsorption column to minimize physicochemical interactions with the metallic parts of the column. Typically, a column packed with small particles (sub-3 μm) is used to enhance efficiency and decrease analysis times. However, instrumentation is critical for modern SEC, and low dispersion UHPLC systems are mandatory. In addition, it is important to consider shear forces, and to adjust flow rates for more fragile molecules. The adoption of monolithic SEC columns would certainly be valuable now that it seems the field is reaching the limits of porous particle SEC. A critical aspect in method development is the selection of appropriate pore size for the stationary phase, based on the hydrodynamic radius of the analyzed molecules. In this context, ultra-wide pore SEC columns (pore size of 1000 Å and beyond) have been developed for the analysis of mRNA, DNA plasmids, viral vectors and lipid nanoparticles.

The capabilities of SEC can be improved thanks to various recent innovations. Employing narrow-bore or even micro-bore SEC columns can enhance MS sensitivity, although the impact of instrumentation becomes more pronounced with such columns. Implementation of recycling SEC is another interesting and relatively easy-to-adopt approach to maximize resolution. SEC can also be particularly interesting in a multidimensional LC setup, since the mobile phase is purely aqueous, which is ideal for combination with RPLC. Finally, a range of informative detectors can be coupled with SEC, including MALS, MS, CDMS or mass photometry.

For the analysis of very large molecules, exceeding 100 or 200 nm in size, SEC may no longer be the best approach. Two alternative size-based chromatographic modes have emerged for such applications. Firstly, there is a re-emergence of interest for hydrodynamic chromatography (HDC), a historical technique originally developed in the 1970′s [201]. In HDC, the separation between molecules of different sizes driven by flowing at different rates through the column, resulting in their elution at distinct times. Larger particles take less time to cross the non-porous

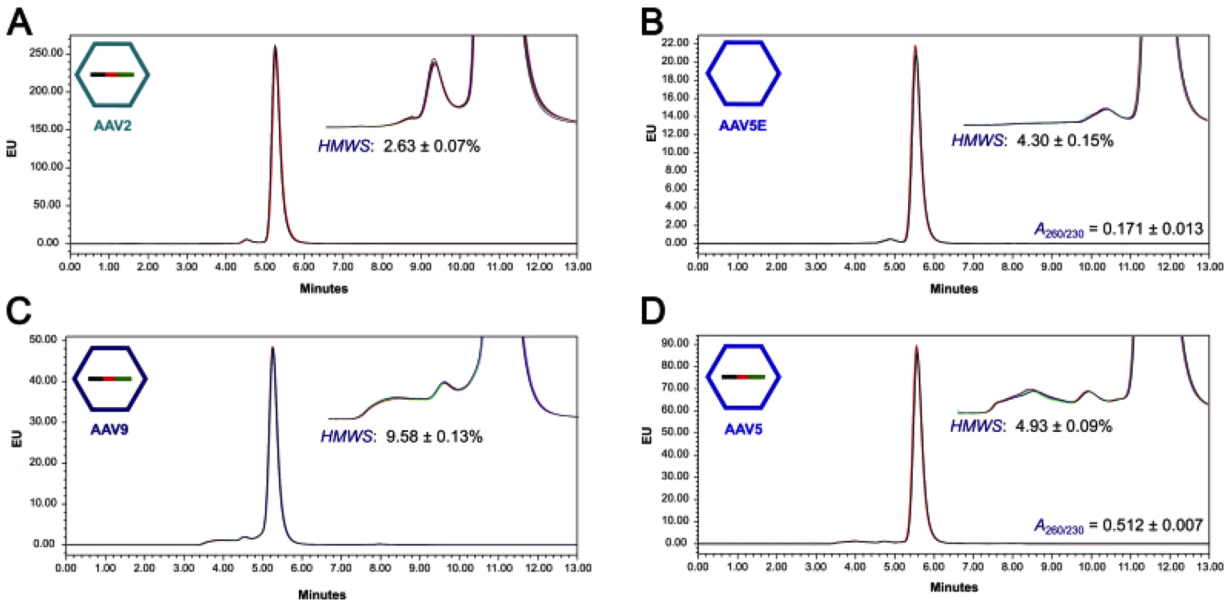

Fig. 18. Overlay of 10 SEC-UV chromatograms for several AAV serotypes (A – AAV2, B – AAV5 empty, C - AAV9, D AAV5 full) showing fast analysis of aggregates for several AAV serotypes using a platform method and a low adsorption 2.5 μm BEH diol 450 Å SEC h-HST Column. Reproduced with permission from [61].

packing, as they can access only the fast flowing channels, resulting in size-based separation [202]. Apart from HDC, it is essential to consider that A4F is also a viable strategy for achieving a size-based separation on very large molecules. Interestingly, A4F has recently been successfully coupled to MS, [203] providing more comprehensive information in a single analysis.

CRediT authorship contribution statement

Valentina D'Atri: Writing – review & editing, Writing – original draft, Funding acquisition. **Mateusz Imiołek:** Writing – review & editing, Writing – original draft. **Colette Quinn:** Writing – review & editing, Writing – original draft. **Abraham Finny:** Writing – original draft. **Matthew Lauber:** Writing – review & editing. **Szabolcs Fekete:** Writing – review & editing, Writing – original draft. **Davy Guillarme:** Writing – review & editing, Writing – original draft, Funding acquisition, Conceptualization.

Declaration of competing interest

The authors declare the following financial interests/personal relationships which may be considered as potential competing interests:

The authors declare the following competing financial interests: Mateusz Imiołek, Colette Quinn, Abraham Finny, Matthew Lauber and Szabolcs Fekete are employees of Waters (Milford, MA, USA), a manufacturer of chromatography systems and consumables.

BEH, XBridge, and IonHance are trademarks of Waters Technologies Corporation. Comirnaty is a trademark of BioNTech SE. Spikevax is a trademark of ModernaTx, Inc. DryLab is a trademark of Molnar, IMRE. Fusion QbD is a trademark of S-Matrix Corporation. ChromSwordAuto is a trademark of ChromSword. AutoChrom is a trademark of Advanced Chemistry Development, Inc. Yarra is a trademark of Phenomenex, Inc. NanoMate is a trademark of Advion, Inc. Sephacryl is a trademark of Cytiva Bioprocess R&D AB. All other marks are the property of their respective owner.

Data availability

Data will be made available on request.

Supplementary materials

Supplementary material associated with this article can be found, in the online version, at doi:10.1016/j.chroma.2024.464862.

References

[1] A.D. Silverman, A.S. Karim, M.C. Jewett, Cell-free gene expression: an expanded repertoire of applications, Nat. Rev. Genet. 21 (2020) 151–170, https://doi.org/10.1038/s41576-019-0186-3.

[2] M.A. Borrelli, H.R. Turnquist, S.R. Little, Biologics and their delivery systems: trends in myocardial infarction, Adv. Drug Deliv. Rev. 173 (2021) 181–215, https://doi.org/10.1016/j.addr.2021.03.014.

[3] R.-M. Lu, Y.-C. Hwang, I.-J. Liu, C.-C. Lee, H.-Z. Tsai, H.-J. Li, H.-C. Wu, Development of therapeutic antibodies for the treatment of diseases, J. Biomed. Sci. 27 (1) (2020), https://doi.org/10.1186/s12929-019-0592-z.

[4] J.K.H. Liu, The history of monoclonal antibody development - progress, remaining challenges and future innovations, Ann. Med. Surg. 3 (2014) 113–116, https://doi.org/10.1016/j.amsu.2014.09.001.

[5] H. Kaplon, A. Chenoweth, S. Crescioli, J.M. Reichert, Antibodies to watch in 2022, MAbs (2022) 14, https://doi.org/10.1080/19420862.2021.2014296.

[6] H. Kaplon, S. Crescioli, A. Chenoweth, J. Visweswaraiah, J.M. Reichert, Antibodies to watch in 2023, MAbs (2023) 15, https://doi.org/10.1080/19420862.2022.2153410.

[7] X. Wu, Z. Gu, Y. Chen, B. Chen, W. Chen, L. Weng, X. Liu, Application of PD-1 blockade in cancer immunotherapy, Comput. Struct. Biotechnol. J. 17 (2019) 661–674, https://doi.org/10.1016/j.csbj.2019.03.006.

[8] K.M. Hargadon, C.E. Johnson, C.J. Williams, Immune checkpoint blockade therapy for cancer: an overview of FDA-approved immune checkpoint inhibitors, Int. Immunopharmacol. 62 (2018) 29–39, https://doi.org/10.1016/j.intimp.2018.06.001.

[9] E. Papanikolaou, A. Bosio, The promise and the hope of gene therapy, Front. Genome Ed. 3 (2021), https://doi.org/10.3389/fgeed.2021.618346.

[10] J.Y. Wang, J.A. Doudna, CRISPR technology: a decade of genome editing is only the beginning, Science (80–) (2023) 379, https://doi.org/10.1126/science.add8643.

[11] M.T.N. Yarnall, E.I. Ioannidi, C. Schmitt-Ulms, R.N. Krajeski, J. Lim, L. Villiger, W. Zhou, K. Jiang, S.K. Garushyants, N. Roberts, L. Zhang, C.A. Vakulskas, J. A. Walker, A.P. Kadina, A.E. Zepeda, K. Holden, H. Ma, J. Xie, G. Gao, L. Foquet, G. Bial, S.K. Donnelly, Y. Miyata, D.R. Radiloff, J.M. Henderson, A. Ujita, O. O. Abudayyeh, J.S. Gootenberg, Drag-and-drop genome insertion of large sequences without double-strand DNA cleavage using CRISPR-directed integrases, Nat. Biotechnol. 41 (2023) 500–512, https://doi.org/10.1038/s41587-022-01527-4.

[12] W.S. Lahr, C.J. Sipe, J.G. Skeate, B.R. Webber, B.S. Moriarity, CRISPR-Cas9 base editors and their current role in human therapeutics, Cytotherapy 25 (2023) 270–276, https://doi.org/10.1016/j.jcyt.2022.11.013.

[13] Cell and Gene therapy (CGT) pipeline deep dive, TuftsMedicine. (2023). https://newdigs.tuftsmedicalcenter.org/payingforcures/defining-disruption/cell-and-gene-therapy-products-and-pipeline/cgt-pipeline-deep-dive/(accessed February 16, 2024).

[14] A. Sparmann, J. Vogel, <scp>RNA</scp>-based medicine: from molecular mechanisms to therapy, EMBO J 42 (2023), https://doi.org/10.15252/embj.2023114760.

[15] J.A. Kulkarni, D. Witzigmann, S.B. Thomson, S. Chen, B.R. Leavitt, P.R. Cullis, R. van der Meel, The current landscape of nucleic acid therapeutics, Nat. Nanotechnol. 16 (2021) 630–643, https://doi.org/10.1038/s41565-021-00898-0.

[16] T.R. Damase, R. Sukhovershin, C. Boada, F. Taraballi, R.I. Pettigrew, J.P. Cooke, The limitless future of RNA therapeutics, Front. Bioeng. Biotechnol. 9 (2021), https://doi.org/10.3389/fbioe.2021.628137.

[17] E. Rohner, R. Yang, K.S. Foo, A. Goedel, K.R. Chien, Unlocking the promise of mRNA therapeutics, Nat. Biotechnol. 40 (2022) 1586–1600, https://doi.org/10.1038/s41587-022-01491-z.

[18] X. Hou, T. Zaks, R. Langer, Y. Dong, Lipid nanoparticles for mRNA delivery, Nat. Rev. Mater. 6 (2021) 1078–1094, https://doi.org/10.1038/s41578-021-00358-0.

[19] R. Tenchov, R. Bird, A.E. Curtze, Q. Zhou, Lipid nanoparticles-from liposomes to mRNA vaccine delivery, a landscape of research diversity and advancement, ACS Nano 15 (2021) 16982–17015, https://doi.org/10.1021/acsnano.1c04996.

[20] Y. Zhu, L. Zhu, X. Wang, H. Jin, RNA-based therapeutics: an overview and prospectus, Cell Death Dis 13 (2022) 644, https://doi.org/10.1038/s41419-022-05075-2.

[21] C.J. Roberts, Protein aggregation and its impact on product quality, Curr. Opin. Biotechnol. 30 (2014) 211–217, https://doi.org/10.1016/j.copbio.2014.08.001.

[22] A. Goyon, S. Tang, S. Fekete, D. Nguyen, K. Hofmann, S. Wang, W. Shatz-Binder, K.I. Fernandez, E.S. Hecht, M. Lauber, K. Zhang, Separation of plasmid DNA topological forms, messenger RNA, and lipid nanoparticle aggregates using an ultrawide pore size exclusion chromatography column, Anal. Chem. 95 (2023) 15017–15024, https://doi.org/10.1021/acs.analchem.3c02944.

[23] I.K. Ventouri, S. Loeber, G.W. Somsen, P.J. Schoenmakers, A. Astefanei, Field-flow fractionation for molecular-interaction studies of labile and complex systems: a critical review, Anal. Chim. Acta 1193 (2022) 339396, https://doi.org/10.1016/j.aca.2021.339396.

[24] S.K. Wiedmer, M.L. Riekkola, Field-flow fractionation - an excellent tool for fractionation, isolation and/or purification of biomacromolecules, J. Chromatogr. A 1712 (2023) 464492, https://doi.org/10.1016/j.chroma.2023.464492.

[25] M. Hee Moon, Flow field-flow fractionation: recent applications for lipidomic and proteomic analysis, TrAC Trends Anal. Chem. 118 (2019) 19–28, https://doi.org/10.1016/j.trac.2019.05.024.

[26] O.J. Valderrama, I. Nischang, Reincarnation of the analytical ultracentrifuge: emerging opportunities for nanomedicine, Anal. Chem. 93 (2021) 15805–15815, https://doi.org/10.1021/acs.analchem.1c03116.

[27] J. Liu, J.D. Andya, S.J. Shire, A critical review of analytical ultracentrifugation and field flow fractionation methods for measuring protein aggregation, AAPS J 8 (2006) E580–E589, https://doi.org/10.1208/aapsj080367.

[28] R. Bhimwal, R.R. Rustandi, A. Payne, M. Dawod, Recent advances in capillary gel electrophoresis for the analysis of proteins, J. Chromatogr. A. 1682 (2022) 463453, https://doi.org/10.1016/j.chroma.2022.463453.

[29] Z. Zhu, J.J. Lu, S. Liu, Protein separation by capillary gel electrophoresis: a review, Anal. Chim. Acta. 709 (2012) 21–31, https://doi.org/10.1016/j.aca.2011.10.022.

[30] L. Hajba, S. Jeong, D.Soo Chung, A. Guttman, Capillary gel electrophoresis of proteins: historical overview and recent advances, TrAC Trends Anal. Chem. 162 (2023) 117024, https://doi.org/10.1016/j.trac.2023.117024.

[31] B.A. Patel, A. Gospodarek, M. Larkin, S.A. Kenrick, M.A. Haverick, N. Tugcu, M. A. Brower, D.D. Richardson, Multi-angle light scattering as a process analytical technology measuring real-time molecular weight for downstream process control, MAbs (2018) 1–6, https://doi.org/10.1080/19420862.2018.1505178.

[32] A. Sharma, J. Beirne, D. Khamar, C. Maguire, A. Hayden, H. Hughes, Evaluation and screening of biopharmaceuticals using multi-angle dynamic light scattering, AAPS PharmSciTech 24 (2023) 84, https://doi.org/10.1208/s12249-023-02529-4.

[33] G. Brusotti, E. Calleri, R. Colombo, G. Massolini, F. Rinaldi, C. Temporini, Advances on size exclusion chromatography and applications on the analysis of

protein biopharmaceuticals and protein aggregates: a mini review, Chromatographia 81 (2018) 3–23, https://doi.org/10.1007/s10337-017-3380-5.
[34] S. Fekete, A. Beck, J. Veuthey, D. Guillarme, Theory and practice of size exclusion chromatography for the analysis of protein aggregates, J. Pharm. Biomed. Anal. 101 (2014) 161–173, https://doi.org/10.1016/j.jpba.2014.04.011.
[35] S. Fekete, A. Goyon, J.-L. Veuthey, D. Guillarme, Size exclusion chromatography of protein biopharmaceuticals: past, present and future, Am. Pharm. Rev. (2018). https://www.americanpharmaceuticalreview.com/Featured-Articles/348912-Size-Exclusion-Chromatography-of-Protein-Biopharmaceuticals-Past-Present-and-Future/.
[36] A. Goyon, D. Guillarme, S. Fekete, The importance of system band broadening in modern size exclusion chromatography, J. Pharm. Biomed. Anal. 135 (2017) 50–60, https://doi.org/10.1016/j.jpba.2016.12.004.
[37] R. Yang, Y. Tang, B. Zhang, X. Lu, A. Liu, Y.T. Zhang, High resolution separation of recombinant monoclonal antibodies by size-exclusion ultra-high performance liquid chromatography (SE-UHPLC), J. Pharm. Biomed. Anal. 109 (2015) 52–61, https://doi.org/10.1016/j.jpba.2015.02.032.
[38] A. Goyon, A. Beck, J.-L. Veuthey, D. Guillarme, S. Fekete, Comprehensive study on the effects of sodium and potassium additives in size exclusion chromatographic separations of protein biopharmaceuticals, J. Pharm. Biomed. Anal. 144 (2017) 242–251, https://doi.org/10.1016/j.jpba.2016.09.031.
[39] S. Fekete, K. Ganzler, D. Guillarme, Critical evaluation of fast size exclusion chromatographic separations of protein aggregates, applying sub-2μm particles, J. Pharm. Biomed. Anal. 78–79 (2013) 141–149, https://doi.org/10.1016/j.jpba.2013.02.013.
[40] A. Goyon, A. Beck, O. Colas, K. Sandra, D. Guillarme, S. Fekete, Evaluation of size exclusion chromatography columns packed with sub-3μm particles for the analysis of biopharmaceutical proteins, J. Chromatogr. A. 1498 (2017) 80–89, https://doi.org/10.1016/j.chroma.2016.11.056.
[41] A. Coffey, G. Staples, Making the most of size-exclusion bioseparations using sub-2-μm column technology, LCGC Eur 33 (2020) 27–36. https://www.chromatographyonline.com/view/making-most-size-exclusion-bioseparations-using-sub-2-m-column-technology-0.
[42] S. Koza, B. Warren, Modern size-exclusion chromatography separations of biosimilar antibodies at physiological pH and ionic strength, Column 18 (2022) 16–21. https://www.chromatographyonline.com/view/modern-size-exclusion-chromatography-separations-of-biosimilar-antibodies-at-physiological-ph-and-ionic-strength.
[43] A. Bhirde, B.V. Chikkaveeraiah, R. Venna, R. Carley, K. Brorson, C. Agarabi, High performance size exclusion chromatography and high-throughput dynamic light scattering as orthogonal methods to screen for aggregation and stability of monoclonal antibody drug products, J. Pharm. Sci. 109 (2020) 3330–3339, https://doi.org/10.1016/j.xphs.2020.08.013.
[44] S. Fekete, D. Guillarme, Influence of connection tubing in modern size exclusion chromatography and its impact on the characterization of mAbs, J. Pharm. Biomed. Anal. 149 (2018) 22–32, https://doi.org/10.1016/j.jpba.2017.10.019.
[45] A.M. Striegel, Multi-detector hydrodynamic chromatography of colloids: following in Hamish Small's footsteps, Heliyon. 7 (2021) e06691. https://doi.org/10.1016/j.heliyon.2021.e06691.
[46] Y.C. Guillaume, F.X. Perrin, C. Guinchard, L. Nicod, T.T. Truong, A. Xicluna, J. Millet, M. Thomassin, Separation in Slalom Chromatography: stretching and Velocity Dependence, Anal. Chem 74 (2002) 1217–1222, https://doi.org/10.1021/ac010852x.
[47] K. Velusamy, Applications of computational fluid dynamics in design of sodium-cooled fast reactors, Adv. Comput. Fluid Dyn. Nucl. React. Des. Saf. Assess. (2019) 729–753, https://doi.org/10.1016/B978-0-08-102337-2.00009-2.
[48] A.M. Striegel, Observations regarding on-column, flow-induced degradation during SEC Analysis, J. Liq. Chromatogr. Relat. Technol. 31 (2008) 3105–3114, https://doi.org/10.1080/10826070802480024.
[49] A.M. Striegel, S.L. Isenberg, G.L. Côté, An SEC/MALS study of alternan degradation during size-exclusion chromatographic analysis, Anal. Bioanal. Chem. 394 (2009) 1887–1893, https://doi.org/10.1007/s00216-009-2895-5.
[50] A.M. Striegel, Do column frits contribute to the on-column, flow-induced degradation of macromolecules? J. Chromatogr. A. 1359 (2014) 147–155, https://doi.org/10.1016/j.chroma.2014.07.033.
[51] Y. Kang, X. Ji, S. Bo, Y. Liu, H. Pasch, Chromatographic mode transition from size exclusion to slalom chromatography as observed for chitosan, Carbohydr. Polym. 235 (2020) 115950, https://doi.org/10.1016/j.carbpol.2020.115950.
[52] N.-S. Cheng, Wall effect on pressure drop in packed beds, Powder Technol 210 (2011) 261–266, https://doi.org/10.1016/j.powtec.2011.03.026.
[53] A. Thaller, L. Schmauder, W. Frieß, G. Winter, T. Menzen, A. Hawe, K. Richter, SV-AUC as a stability-indicating method for the characterization of mRNA-LNPs, Eur. J. Pharm. Biopharm. 182 (2023) 152–156, https://doi.org/10.1016/j.ejpb.2022.11.014.
[54] B. Fongaro, B. Campara, G.Y. Moscatiello, A. De Luigi, D. Panzeri, L. Sironi, P. Bigini, G. Carretta, G. Miolo, G. Pasut, P. Polverino De Laureto, Assessing the physicochemical stability and intracellular trafficking of mRNA-based COVID-19 vaccines, Int. J. Pharm. 644 (2023) 123319, https://doi.org/10.1016/j.ijpharm.2023.123319.
[55] F. Gritti, J. Hochstrasser, A. Svidrytski, D. Hlushkou, U. Tallarek, Morphology-transport relationships in liquid chromatography: application to method development in size exclusion chromatography, J. Chromatogr. A. 1620 (2020) 460991, https://doi.org/10.1016/j.chroma.2020.460991.
[56] J.C. Giddings, E. Kucera, C.P. Russell, M.N. Myers, Statistical theory for the equilibrium distribution of rigid molecules in inert porous networks. Exclusion chromatography, J. Phys. Chem. 72 (1968) 4397–4408, https://doi.org/10.1021/j100859a008.
[57] Y. Vander Heyden, S.T. Popovici, P.J. Schoenmakers, Evaluation of size-exclusion chromatography and size-exclusion electrochromatography calibration curves, J. Chromatogr. A. 957 (2002) 127–137, https://doi.org/10.1016/S0021-9673(02)00311-4.
[58] J.E. Harlan, D. Picot, P.J. Loll, R.M. Garavito, Calibration of size-exclusion chromatography: use of a double gaussian distribution function to describe pore sizes, Anal. Biochem. 224 (1995) 557–563, https://doi.org/10.1006/abio.1995.1087.
[59] A. Oliva, M. Llabrés, J.B. Fariña, Comparative study of protein molecular weights by size-exclusion chromatography and laser-light scattering, J. Pharm. Biomed. Anal. 25 (2001) 833–841, https://doi.org/10.1016/S0731-7085(01)00359-4.
[60] S. Fekete, M. Lauber, M. Xu, Considering the selectivity of pore size gradient size exclusion chromatography columns, J. Chromatogr. A. 1718 (2024) 464726, https://doi.org/10.1016/j.chroma.2024.464726.
[61] M. Imiołek, S. Fekete, L. Kizekai, B. Addepalli, M. Lauber, Fast and efficient size exclusion chromatography of adeno associated viral vectors with 2.5 micrometer particle low adsorption columns, J. Chromatogr. A. 1714 (2024) 464587, https://doi.org/10.1016/j.chroma.2023.464587.
[62] H. Meng, M. Sorrentino, D. Woodcock, C. O'Riordan, V. Dhawan, M. Verhagen, C. Davies, Size exclusion chromatography with dual wavelength detection as a sensitive and accurate method for determining the empty and full capsids of recombinant adeno-associated viral vectors, Hum. Gene Ther 33 (2022) 202–212, https://doi.org/10.1089/hum.2021.123.
[63] J. Zhang, R.M. Haas, A.M. Leone, Polydispersity characterization of lipid nanoparticles for siRNA delivery using multiple detection size-exclusion chromatography, Anal. Chem. 84 (2012) 6088–6096, https://doi.org/10.1021/ac3007768.
[64] M. Gilar, C. Doneanu, M.M. Gaye, Liquid chromatography methods for analysis of mRNA Poly(A) tail length and heterogeneity, Anal. Chem. 95 (2023) 14308–14316, https://doi.org/10.1021/acs.analchem.3c02552.
[65] B. Kempf, R. Eksteen, The Effect of SEC column arrangement of different pore sizes on resolution and molecular weight measurements, LCGC North Am 29 (2011) 668–671. https://www.chromatographyonline.com/view/effect-sec-column-arrangement-different-pore-sizes-resolution-and-molecular-weight-measurements.
[66] S. Koza, K.J. Fountain, Waters application note 720004618EN - advances in size exclusion chromatography for the analysis of macromolecular proteins, (2013). https://www.waters.com/webassets/cms/library/docs/720004618en.pdf.
[67] F. Gritti, Theoretical performance of multiple size-exclusion chromatography columns connected in series, J. Chromatogr. A. 1634 (2020) 461673, https://doi.org/10.1016/j.chroma.2020.461673.
[68] B. Sreedhar, A. Seidel-Morgenstern, Preparative separation of multi-component mixtures using stationary phase gradients, J. Chromatogr. A. 1215 (2008) 133–144, https://doi.org/10.1016/j.chroma.2008.11.003.
[69] M. Kuehnle, J. Rehbein, K. Holtin, B. Dietrich, M. Gradl, H. Yeman, K. Albert, Phase optimized liquid chromatography as an instrument for steroid analysis, J. Sep. Sci. 31 (2008) 1655–1661, https://doi.org/10.1002/jssc.200700604.
[70] Y. Yang, M. Li, Y. Zhao, X. Lin, Z. Su, F. Xin, X. Du, K. Zheng, R. Han, Y. Pan, S. He, S. Zhang, Mechanism and inhibition of abnormal chromatographic behavior of serotype type a inactivated foot and mouth disease virus in high-performance size-exclusion chromatography, J. Chromatogr. A. 1686 (2022) 463648, https://doi.org/10.1016/j.chroma.2022.463648.
[71] W. Li, B.A. Persson, M. Morin, M.A. Behrens, M. Lund, M.Zackrisson Oskolkova, Charge-induced patchy attractions between proteins, J. Phys. Chem. B. 119 (2015) 503–508, https://doi.org/10.1021/jp512027j.
[72] M.E. Reinau, D. Åsberg, Characterization of antibody surface properties and selection of a diverse subset for development of a generic size-exclusion chromatography method, J. Chromatogr. A. 1716 (2024) 464652, https://doi.org/10.1016/j.chroma.2024.464652.
[73] T. Arakawa, D. Ejima, T. Li, J.S. Philo, The critical role of mobile phase composition in size exclusion chromatography of protein pharmaceuticals, J. Pharm. Sci. 99 (2010) 1674–1692, https://doi.org/10.1002/jps.21974.
[74] A. Wakamatsu, K. Morimoto, M. Shimizu, S. Kudoh, A severe peak tailing of phosphate compounds caused by interaction with stainless steel used for liquid chromatography and electrospray mass spectrometry, J. Sep. Sci. 28 (2005) 1823–1830, https://doi.org/10.1002/jssc.200400027.
[75] A. Goyon, M. Excoffier, M.C. Janin Bussat, B. Bobaly, S. Fekete, D. Guillarme, A. Beck, Determination of isoelectric points and relative charge variants of 23 therapeutic monoclonal antibodies, J. Chromatogr. B. 1066 (2017) 119–128, https://doi.org/10.1016/j.jchromb.2017.09.033.
[76] A. Méndez, E. Bosch, M. Rosés, U.D. Neue, Comparison of the acidity of residual silanol groups in several liquid chromatography columns, J. Chromatogr. A. 986 (2003) 33–44, https://doi.org/10.1016/S0021-9673(02)01899-X.
[77] S. Fekete, L. Kizekai, Y.T. Sarisozen, N. Lawrence, S. Shiner, M. Lauber, Investigating the secondary interactions of packing materials for size-exclusion chromatography of therapeutic proteins, J. Chromatogr. A. 1676 (2022) 463262, https://doi.org/10.1016/j.chroma.2022.463262.
[78] R. Knihtila, Y. Song, L. Chemmalil, J. Ding, N. Mussa, Z.J. Li, Systematic development of a size exclusion chromatography method for a monoclonal antibody with high surface aggregation propensity (SAP) index, J. Pharm. Sci. 110 (2021) 2651–2660, https://doi.org/10.1016/j.xphs.2021.03.023.
[79] A. Goyon, L. Sciascera, A. Clarke, D. Guillarme, R. Pell, Extending the limits of size exclusion chromatography: simultaneous separation of free payloads and related species from antibody drug conjugates and their aggregates,

J. Chromatogr. A. 1539 (2018) 19–29, https://doi.org/10.1016/j.chroma.2018.01.039.
[80] H. Wang, M.S. Levi, A.V. Del Grosso, W.M. McCormick, L. Bhattacharyya, An improved size exclusion-HPLC method for molecular size distribution analysis of immunoglobulin G using sodium perchlorate in the eluent, J. Pharm. Biomed. Anal. 138 (2017) 330–343, https://doi.org/10.1016/j.jpba.2017.02.025.
[81] R. Yumioka, H. Sato, H. Tomizawa, Y. Yamasaki, D. Ejima, Mobile phase containing arginine provides more reliable SEC condition for aggregation analysis, J. Pharm. Sci. 99 (2010) 618–620, https://doi.org/10.1002/jps.21857.
[82] D. Wang, C. Nowak, B. Mason, A. Katiyar, H. Liu, Analytical artifacts in characterization of recombinant monoclonal antibody therapeutics, J. Pharm. Biomed. Anal. 183 (2020) 113131, https://doi.org/10.1016/j.jpba.2020.113131.
[83] B. Duivelshof, A. Zöldhegyi, D. Guillarme, M. Lauber, S. Fekete, Expediting the chromatographic analysis of COVID-19 antibody therapeutics with ultra-short columns, retention modeling and automated method development, J. Pharm. Biomed. Anal. 221 (2022) 115039, https://doi.org/10.1016/j.jpba.2022.115039.
[84] E.S.P. Bouvier, S.M. Koza, Advances in size-exclusion separations of proteins and polymers by UHPLC, TrAC Trends Anal. Chem. 63 (2014) 85–94, https://doi.org/10.1016/j.trac.2014.08.002.
[85] S. Fekete, M.A. Lauber, Waters Application Note 720007790 - Method Development Approach to Optimize Protein Size Exclusion Chromatography, (2022).
[86] R. Verseput, Fusion <scp>QbD</scp>® software implementation of <scp>APLM</scp>best practices for analytical method development, validation, and transfer, Optim. HPLC, Wiley (2021) 199–218, https://doi.org/10.1002/9783527837489.ch2-2.
[87] L. Mondello, Szabolcs Fekete, Imre Molnár, Software-assisted method development in high performance liquid chromatography, Anal. Bioanal. Chem. 411 (2019) 3707–3708, https://doi.org/10.1007/s00216-019-01855-6.
[88] D. Some, Waters | Wyatt Technology White Paper WP1615 - SEC-MALS for absolute biophysical characterization, (2024). https://wyattfiles.s3-us-west-2.amazonaws.com/literature/white-papers/WP1615-SEC-MALS-for-absolute-biophysical-characterization.pdf.
[89] D. Some, V. Razinkov, High-Throughput Analytical Light Scattering for Protein Quality Control and Characterization, in: 2019: pp. 335–359. https://doi.org/10.1007/978-1-4939-9624-7_16.
[90] P.J. Wyatt, Light scattering and the absolute characterization of macromolecules, Anal. Chim. Acta. 272 (1993) 1–40. https://ahgroup.at/user_files/_References/AF4_MALLS-Wyatt_AnalyticaChmicaActa_272_1-40_1993.pdf.
[91] D. Some, S. Kenrick, Characterization of protein-protein interactions via static and dynamic light scattering. Protein Interact, InTech, 2012, https://doi.org/10.5772/37240.
[92] B.S. Kendrick, B.A. Kerwin, B.S. Chang, J.S. Philo, Online size-exclusion high-performance liquid chromatography light scattering and differential refractometry methods to determine degree of polymer conjugation to proteins and protein–protein or protein–ligand association states, Anal. Biochem. 299 (2001) 136–146, https://doi.org/10.1006/abio.2001.5411.
[93] J. Philo, A critical review of methods for size characterization of non-particulate protein aggregates, Curr. Pharm. Biotechnol. 10 (2009) 359–372, https://doi.org/10.2174/138920109788488815.
[94] B. Troxell, I.-W. Tsai, K. Shah, C.I. Knuckles, S. Shelton, K. Lindsey, S.M. B. Cardenas, T. Roberts, Application of size exclusion chromatography with multiangle light scattering in the analytical development of a preclinical stage gene therapy program, Hum. Gene Ther. 34 (2023) 325–338, https://doi.org/10.1089/hum.2022.218.
[95] J. De Vos, P.Pereira Aguilar, C. Köppl, A. Fischer, C. Grünwald-Gruber, M. Dürkop, M. Klausberger, J. Mairhofer, G. Striedner, M. Cserjan-Puschmann, A. Jungbauer, N. Lingg, Production of full-length SARS-CoV-2 nucleocapsid protein from Escherichia coli optimized by native hydrophobic interaction chromatography hyphenated to multi-angle light scattering detection, Talanta 235 (2021) 122691, https://doi.org/10.1016/j.talanta.2021.122691.
[96] A. Äärelä, K. Räsänen, P. Holm, H. Salo, P. Virta, Synthesis of site-specific antibody–[60]fullerene–oligonucleotide conjugates for cellular targeting, ACS Appl. Bio Mater. 6 (2023) 3189–3198, https://doi.org/10.1021/acsabm.3c00318.
[97] P. Legrand, S. Dufaÿ, N. Mignet, P. Houzé, R. Gahoual, Modeling study of long-term stability of the monoclonal antibody infliximab and biosimilars using liquid-chromatography–tandem mass spectrometry and size-exclusion chromatography–multi-angle light scattering, Anal. Bioanal. Chem. 415 (2023) 179–192, https://doi.org/10.1007/s00216-022-04396-7.
[98] E. Lubomirsky, A. Khodabandeh, J. Preis, M. Susewind, T. Hofe, E.F. Hilder, R. D. Arrua, Polymeric stationary phases for size exclusion chromatography: a review, Anal. Chim. Acta. 1151 (2021) 338244, https://doi.org/10.1016/j.aca.2021.338244.
[99] J.C. Rea, Y. Lou, J. Cuzzi, Y. Hu, I. de Jong, Y.J. Wang, D. Farnan, Development of capillary size exclusion chromatography for the analysis of monoclonal antibody fragments extracted from human vitreous humor, J. Chromatogr. A. 1270 (2012) 111–117, https://doi.org/10.1016/j.chroma.2012.10.051.
[100] J.C. Rea, G.T. Moreno, L. Vampola, Y. Lou, B. van Haan, G. Tremintin, L. Simmons, A. Nava, Y.J. Wang, D. Farnan, Capillary size exclusion chromatography with picogram sensitivity for analysis of monoclonal antibodies purified from harvested cell culture fluid, J. Chromatogr. A. 1219 (2012) 140–146, https://doi.org/10.1016/j.chroma.2011.11.025.
[101] E. Hecht, E. Obiorah, X. Liu, L. Morrison, H. Shion, M. Lauber, Microflow size exclusion chromatography to preserve micromolar affinity complexes and achieve subunit separations for native state mass spectrometry, J. Chromatogr. A. 1685 (2022) 463638, https://doi.org/10.1016/j.chroma.2022.463638.
[102] S. Fekete, M. Lauber, Insights on further improving fast size exclusion chromatography separations of biopharmaceuticals using 2.1 mm column diameters, J. Chromatogr. A. 1690 (2023) 463810, https://doi.org/10.1016/j.chroma.2023.463810.
[103] M. DeLano, T.H. Walter, M.A. Lauber, M. Gilar, M.C. Jung, J.M. Nguyen, C. Boissel, A.V. Patel, A. Bates-Harrison, K.D. Wyndham, Using hybrid organic–inorganic surface technology to mitigate analyte interactions with metal surfaces in UHPLC, Anal. Chem. 93 (2021) 5773–5781, https://doi.org/10.1021/acs.analchem.0c05203.
[104] M. Gilar, M. DeLano, F. Gritti, Mitigation of analyte loss on metal surfaces in liquid chromatography, J. Chromatogr. A. 1650 (2021) 462247, https://doi.org/10.1016/j.chroma.2021.462247.
[105] P. Hambleton, W.J. Lough, J. Maltas, M.J. Mills, Unusual analyte adsorption effects on inert Lc components, J. Liq. Chromatogr. 18 (1995) 3205–3217, https://doi.org/10.1080/10826079508010445.
[106] S. Fekete, M. DeLano, A.B. Harrison, S.J. Shiner, J.L. Belanger, K.D. Wyndham, M. A. Lauber, Size exclusion and ion exchange chromatographic hardware modified with a hydrophilic hybrid surface, Anal. Chem. 94 (2022) 3360–3367, https://doi.org/10.1021/acs.analchem.1c05466.
[107] N.L. McIntosh, G.Y. Berguig, O.A. Karim, C.L. Cortesio, R. De Angelis, A.A. Khan, D. Gold, J.A. Maga, V.S. Bhat, Author correction: comprehensive characterization and quantification of adeno associated vectors by size exclusion chromatography and multi angle light scattering, Sci. Rep. 12 (2022) 19754, https://doi.org/10.1038/s41598-022-23249-y.
[108] K.J. Hassett, J. Higgins, A. Woods, B. Levy, Y. Xia, C.J. Hsiao, E. Acosta, Ö. Almarsson, M.J. Moore, L.A. Brito, Impact of lipid nanoparticle size on mRNA vaccine immunogenicity, J. Control. Release. 335 (2021) 237–246, https://doi.org/10.1016/j.jconrel.2021.05.021.
[109] M. Tsoi, T.T. Do, V. Tang, J.A. Aguilera, C.C. Perry, J.R. Milligan, Characterization of condensed plasmid DNA models for studying the direct effect of ionizing radiation, Biophys. Chem. 147 (2010) 104–110, https://doi.org/10.1016/j.bpc.2009.12.006.
[110] J.D. Rubin, T.V. Nguyen, K.L. Allen, K. Ayasoufi, M.A. Barry, Comparison of gene delivery to the kidney by adenovirus, adeno-associated virus, and lentiviral vectors after intravenous and direct kidney injections, Hum. Gene Ther. 30 (2019) 1559–1571, https://doi.org/10.1089/hum.2019.127.
[111] Y.-Z. Tan, L.-Z. Qiao, S.-S. Wang, J. Zhang, J. Qian, M. Zhu, S.-J. Yao, D.-Q. Lin, Enhanced adsorption performance of varying-length mRNA on Oligo dT affinity resins through optimal pore size and grafting, Biochem. Eng. J. 203 (2024) 109213, https://doi.org/10.1016/j.bej.2023.109213.
[112] D. Some, H. Amartely, A. Tsadok, M. Lebendiker, Characterization of proteins by size-exclusion chromatography coupled to multi-angle light scattering (SEC-MALS), J. Vis. Exp. (2019), https://doi.org/10.3791/59615.
[113] J. PORATH, H. BENNICH, Recycling chromatography, Arch. Biochem. Biophys. Suppl 1 (1962) 152–156. http://www.ncbi.nlm.nih.gov/pubmed/13972318.
[114] F. Gritti, M. Leal, T. McDonald, M. Gilar, Ideal versus real automated twin column recycling chromatography process, J. Chromatogr. A. 1508 (2017) 81–94, https://doi.org/10.1016/j.chroma.2017.06.009.
[115] F. Gritti, S. Besner, S. Cormier, M. Gilar, Applications of high-resolution recycling liquid chromatography: from small to large molecules, J. Chromatogr. A. 1524 (2017) 108–120, https://doi.org/10.1016/j.chroma.2017.09.054.
[116] M. Haberger, M. Leiss, A.-K. Heidenreich, O. Pester, G. Hafenmair, M. Hook, L. Bonnington, H. Wegele, M. Haindl, D. Reusch, P. Bulau, Rapid characterization of biotherapeutic proteins by size-exclusion chromatography coupled to native mass spectrometry, MAbs 8 (2016) 331–339, https://doi.org/10.1080/19420862.2015.1122150.
[117] A. Goyon, V. D'Atri, O. Colas, S. Fekete, A. Beck, D. Guillarme, Characterization of 30 therapeutic antibodies and related products by size exclusion chromatography: feasibility assessment for future mass spectrometry hyphenation, J. Chromatogr. B. 1065–1066 (2017) 35–43, https://doi.org/10.1016/j.jchromb.2017.09.027.
[118] Z.L. VanAernum, F. Busch, B.J. Jones, M. Jia, Z. Chen, S.E. Boyken, A. Sahasrabuddhe, D. Baker, V.H. Wysocki, Rapid online buffer exchange for screening of proteins, protein complexes and cell lysates by native mass spectrometry, Nat. Protoc. 15 (2020) 1132–1157, https://doi.org/10.1038/s41596-019-0281-0.
[119] I.K. Ventouri, D.B.A. Malheiro, R.L.C. Voeten, S. Kok, M. Honing, G.W. Somsen, R. Haselberg, Probing protein denaturation during size-exclusion chromatography using native mass spectrometry, Anal. Chem. 92 (2020) 4292–4300, https://doi.org/10.1021/acs.analchem.9b04961.
[120] J.B. Hedges, S. Vahidi, X. Yue, L. Konermann, Effects of ammonium bicarbonate on the electrospray mass spectra of proteins: evidence for bubble-induced unfolding, Anal. Chem. 85 (2013) 6469–6476, https://doi.org/10.1021/ac401020s.
[121] A. Murisier, S. Fekete, D. Guillarme, V. D'Atri, The importance of being metal-free: the critical choice of column hardware for size exclusion chromatography coupled to high resolution mass spectrometry, Anal. Chim. Acta. 1183 (2021) 338987, https://doi.org/10.1016/j.aca.2021.338987.
[122] A. Murisier, M. Andrie, S. Fekete, M. Lauber, V. D'Atri, K. Iwan, D. Guillarme, Direct coupling of size exclusion chromatography and mass spectrometry for the characterization of complex monoclonal antibody products, J. Sep. Sci. 45 (2022) 1997–2007, https://doi.org/10.1002/jssc.202200075.
[123] I.K. Ventouri, S. Veelders, M. Passamonti, P. Endres, R. Roemling, P. J. Schoenmakers, G.W. Somsen, R. Haselberg, A.F.G. Gargano, Micro-flow size-

exclusion chromatography for enhanced native mass spectrometry of proteins and protein complexes, Anal. Chim. Acta. 1266 (2023) 341324, https://doi.org/10.1016/j.aca.2023.341324.
[124] Mass photometry supports AAV production and purification processes, (2023). https://www.refeyn.com/aav-production-and-purification (accessed February 16, 2024).
[125] T.P. Wörner, J. Snijder, A. Bennett, M. Agbandje-McKenna, A.A. Makarov, A.J. R. Heck, Resolving heterogeneous macromolecular assemblies by Orbitrap-based single-particle charge detection mass spectrometry, Nat. Methods. 17 (2020) 395–398, https://doi.org/10.1038/s41592-020-0770-7.
[126] V.U. Weiss, K. Wieland, A. Schwaighofer, B. Lendl, G. Allmaier, Native nano-electrospray differential mobility analyzer (nES GEMMA) enables size selection of liposomal nanocarriers combined with subsequent direct spectroscopic analysis, Anal. Chem. 91 (2019) 3860–3868, https://doi.org/10.1021/acs.analchem.8b04252.
[127] S. Steinberger, S. Karuthedom George, L. Lauková, R. Weiss, C. Tripisciano, M. Marchetti-Deschmann, V. Weber, G. Allmaier, V.U. Weiss, Targeting the structural integrity of extracellular vesicles via nano electrospray gas-phase electrophoretic mobility molecular analysis (nES GEMMA), Membranes (Basel) 12 (2022) 872, https://doi.org/10.3390/membranes12090872.
[128] V.U. Weiss, K. Balantic, E. Pittenauer, C. Tripisciano, G. Friedbacher, V. Weber, M. Marchetti-Deschmann, G. Allmaier, Nano electrospray differential mobility analysis based size-selection of liposomes and very-low density lipoprotein particles for offline hyphenation to MALDI mass spectrometry, J. Pharm. Biomed. Anal. 179 (2020) 112998, https://doi.org/10.1016/j.jpba.2019.112998.
[129] S.-H. Lai, S. Tamara, A.J.R. Heck, Single-particle mass analysis of intact ribosomes by mass photometry and Orbitrap-based charge detection mass spectrometry, IScience 24 (2021) 103211, https://doi.org/10.1016/j.isci.2021.103211.
[130] T.P. Wörner, T.M. Shamorkina, J. Snijder, A.J.R. Heck, Mass spectrometry-based structural virology, Anal. Chem. 93 (2021) 620–640, https://doi.org/10.1021/acs.analchem.0c04339.
[131] J.O. Kafader, R.D. Melani, K.R. Durbin, B. Ikwuagwu, B.P. Early, R.T. Fellers, S. C. Beu, V. Zabrouskov, A.A. Makarov, J.T. Maze, D.L. Shinholt, P.F. Yip, D. Tullman-Ercek, M.W. Senko, P.D. Compton, N.L. Kelleher, Multiplexed mass spectrometry of individual ions improves measurement of proteoforms and their complexes, Nat. Methods. 17 (2020) 391–394, https://doi.org/10.1038/s41592-020-0764-5.
[132] D.Z. Keifer, E.E. Pierson, M.F. Jarrold, Charge detection mass spectrometry: weighing heavier things, Analyst 142 (2017) 1654–1671, https://doi.org/10.1039/C7AN00277G.
[133] T.P. Wörner, J. Snijder, O. Friese, T. Powers, A.J.R. Heck, Assessment of genome packaging in AAVs using orbitrap-based charge-detection mass spectrometry, Mol. Ther. - Methods Clin. Dev. 24 (2022) 40–47, https://doi.org/10.1016/j.omtm.2021.11.013.
[134] J.P. McGee, R.D. Melani, P.F. Yip, M.W. Senko, P.D. Compton, J.O. Kafader, N. L. Kelleher, Isotopic resolution of protein complexes up to 466kDa using individual ion mass spectrometry, Anal. Chem. 93 (2021) 2723–2727, https://doi.org/10.1021/acs.analchem.0c03282.
[135] F. Soltermann, E.D.B. Foley, V. Pagnoni, M. Galpin, J.L.P. Benesch, P. Kukura, W. B. Struwe, Quantifying protein–protein interactions by molecular counting with mass photometry, Angew. Chemie. 132 (2020) 10866–10871, https://doi.org/10.1002/ange.202001578.
[136] A. Sonn-Segev, K. Belacic, T. Bodrug, G. Young, R.T. VanderLinden, B. A. Schulman, J. Schimpf, T. Friedrich, P.V. Dip, T.U. Schwartz, B. Bauer, J.-M. Peters, W.B. Struwe, J.L.P. Benesch, N.G. Brown, D. Haselbach, P. Kukura, Quantifying the heterogeneity of macromolecular machines by mass photometry, Nat. Commun. 11 (2020) 1772, https://doi.org/10.1038/s41467-020-15642-w.
[137] G. Young, N. Hundt, D. Cole, A. Fineberg, J. Andrecka, A. Tyler, A. Olerinyova, A. Ansari, E.G. Marklund, M.P. Collier, S.A. Chandler, O. Tkachenko, J. Allen, M. Crispin, N. Billington, Y. Takagi, J.R. Sellers, C. Eichmann, P. Selenko, L. Frey, R. Riek, M.R. Galpin, W.B. Struwe, J.L.P. Benesch, P. Kukura, Quantitative mass imaging of single biological macromolecules, Science 360 (80–) (2018) 423–427, https://doi.org/10.1126/science.aar5839.
[138] A.E. Grande, X. Li, L.M. Miller, J. Zhang, B.E. Draper, R.W. Herzog, W. Xiao, M. F. Jarrold, Antibody binding to recombinant adeno associated virus monitored by charge detection mass spectrometry, Anal. Chem. 95 (2023) 10864–10868, https://doi.org/10.1021/acs.analchem.3c02371.
[139] S.D. Fuerstenau, W.H. Benner, Molecular weight determination of megadalton DNA electrospray ions using charge detection time-of-flight mass spectrometry, Rapid Commun. Mass Spectrom. 9 (1995) 1528–1538, https://doi.org/10.1002/rcm.1290091513.
[140] L.F. Barnes, B.E. Draper, J. Kurian, Y.-T. Chen, T. Shapkina, T.W. Powers, M. F. Jarrold, Analysis of AAV-Extracted DNA by charge detection mass spectrometry reveals genome truncations, Anal. Chem. 95 (2023) 4310–4316, https://doi.org/10.1021/acs.analchem.2c04234.
[141] M.A. den Boer, S.-H. Lai, X. Xue, M.D. van Kampen, B. Bleijlevens, A.J.R. Heck, Comparative analysis of antibodies and heavily glycosylated macromolecular immune complexes by size-exclusion chromatography multi-angle light scattering, native charge detection mass spectrometry, and mass photometry, Anal. Chem. 94 (2022) 892–900, https://doi.org/10.1021/acs.analchem.1c03656.
[142] D. Wu, X. Zhao, D.A. Jimenez, G. Piszczek, Size exclusion chromatography–mass photometry: a new method for adeno-associated virus product characterization, Cells 12 (2023) 2264, https://doi.org/10.3390/cells12182264.
[143] D. Wu, P. Hwang, T. Li, G. Piszczek, Rapid characterization of adeno-associated virus (AAV) gene therapy vectors by mass photometry, Gene Ther. 29 (2022) 691–697, https://doi.org/10.1038/s41434-021-00311-4.
[144] A. Viodé, X. Dagany, M. Kerleroux, P. Dugourd, T. Doussineau, L. Charles, R. Antoine, Coupling of size-exclusion chromatography with electrospray ionization charge-detection mass spectrometry for the characterization of synthetic polymers of ultra-high molar mass, Rapid Commun. Mass Spectrom. 30 (2016) 132–136, https://doi.org/10.1002/rcm.7426.
[145] L. Strasser, F. Füssl, T.E. Morgan, S. Carillo, J. Bones, Exploring charge-detection mass spectrometry on chromatographic time scales, Anal. Chem. 95 (2023) 15118–15124, https://doi.org/10.1021/acs.analchem.3c03325.
[146] A. Williams, E.K. Read, C.D. Agarabi, S. Lute, K.A. Brorson, Automated 2D-HPLC method for characterization of protein aggregation with in-line fraction collection device, J. Chromatogr. B. 1046 (2017) 122–130, https://doi.org/10.1016/j.jchromb.2017.01.021.
[147] Z.D. Dunn, J. Desai, G.M. Leme, D.R. Stoll, D.D. Richardson, Rapid two-dimensional Protein-A size exclusion chromatography of monoclonal antibodies for titer and aggregation measurements from harvested cell culture fluid samples, MAbs (2020) 12, https://doi.org/10.1080/19420862.2019.1702263.
[148] Y. A, S. V, C. Y, Y. S, Z. Y, K. S, M. S, R. D, C. Z, Forced degradation study of monoclonal antibody using two- dimensional liquid chromatography, J. Chromatogr. Sep. Tech. (2017) 08, https://doi.org/10.4172/2157-7064.1000365.
[149] G. Lambiase, S.E. Inman, M. Muroni, V. Lindo, M.J. Dickman, D.C. James, High-throughput multiplex analysis of mAb aggregates and charge variants by automated two-dimensional size exclusion-cation exchange chromatography coupled to mass spectrometry, J. Chromatogr. A. 1670 (2022) 462944, https://doi.org/10.1016/j.chroma.2022.462944.
[150] A. Goyon, M. Kim, L. Dai, C. Cornell, F. Jacobson, D. Guillarme, C. Stella, Streamlined characterization of an antibody-drug conjugate by two-dimensional and four-dimensional liquid chromatography/mass spectrometry, Anal. Chem. (2019), https://doi.org/10.1021/acs.analchem.9b02454.
[151] A. Ehkirch, V. D'Atri, F. Rouviere, O. Hernandez-Alba, A. Goyon, O. Colas, M. Sarrut, A. Beck, D. Guillarme, S. Heinisch, S. Cianferani, An online four-dimensional HIC×SEC-IM×MS methodology for proof-of-concept characterization of antibody drug conjugates, Anal. Chem. 90 (2018) 1578–1586, https://doi.org/10.1021/acs.analchem.7b02110.
[152] A. Ehkirch, A. Goyon, O. Hernandez-Alba, F. Rouviere, V. D'Atri, C. Dreyfus, J.-F. Haeuw, H. Diemer, A. Beck, S. Heinisch, D. Guillarme, S. Cianferani, A novel online four-dimensional SEC×SEC-IM×MS methodology for characterization of monoclonal antibody size variants, Anal. Chem. 90 (2018) 13929–13937, https://doi.org/10.1021/acs.analchem.8b03333.
[153] L. Verscheure, G. Vanhoenacker, S. Schneider, T. Merchiers, J. Storms, P. Sandra, F. Lynen, K. Sandra, 3D-LC-MS with 2 D multimethod option for fully automated assessment of multiple attributes of monoclonal antibodies directly from cell culture supernatants, Anal. Chem. 94 (2022) 6502–6511, https://doi.org/10.1021/acs.analchem.1c05461.
[154] R. Sadighi, V. de Kleijne, S. Wouters, K. Lubbers, G.W. Somsen, A.F.G. Gargano, R. Haselberg, Online multimethod platform for comprehensive characterization of monoclonal antibodies in cell culture fluid from a single sample injection - intact protein workflow, Anal. Chim. Acta. 1287 (2024) 342074, https://doi.org/10.1016/j.aca.2023.342074.
[155] R.R. Burgess, A brief practical review of size exclusion chromatography: rules of thumb, limitations, and troubleshooting, Protein Expr. Purif. 150 (2018) 81–85, https://doi.org/10.1016/j.pep.2018.05.007.
[156] M.C. Nweke, R.G. McCartney, D.G. Bracewell, Mechanical characterisation of agarose-based chromatography resins for biopharmaceutical manufacture, J. Chromatogr. A. 1530 (2017) 129–137, https://doi.org/10.1016/j.chroma.2017.11.038.
[157] M.C. Nweke, A.S. Rathore, D.G. Bracewell, Lifetime and aging of chromatography resins during biopharmaceutical manufacture, Trends Biotechnol 36 (2018) 992–995, https://doi.org/10.1016/j.tibtech.2018.01.001.
[158] Y. Xu, S. Pan, R. Ghosh, A new approach for increasing speed, loading capacity, resolution, and scalability of preparative size-exclusion chromatography of proteins, Processes 10 (2022) 2566, https://doi.org/10.3390/pr10122566.
[159] R. Ghosh, G. Hale, Y. Durocher, P. Gatt, Dry-compression packing of hydroxyapatite nanoparticles within a flat cuboid chromatography device and its use for fast protein separation, J. Chromatogr. A. 1667 (2022) 462881, https://doi.org/10.1016/j.chroma.2022.462881.
[160] R. Ghosh, G. Chen, U. Umatheva, P. Gatt, A flow distribution and collection feature for ensuring scalable uniform flow in a chromatography device, J. Chromatogr. A. 1618 (2020) 460892, https://doi.org/10.1016/j.chroma.2020.460892.
[161] G. Chen, R. Roshankhah, R. Ghosh, A cuboid chromatography device having short bed-height gives better protein separation at a significantly lower pressure drop than a taller column having the same bed-volume, J. Chromatogr. A. 1647 (2021) 462167, https://doi.org/10.1016/j.chroma.2021.462167.
[162] Monograph <129>Analytical Procedures For Recombinat Therapeutic Monoclonal Antibodies, U.S. Pharmacop. (2017).
[163] B. Boulanger, E. Rozet, F. Moonen, S. Rudaz, P. Hubert, A risk-based analysis of the AAPS conference report on quantitative bioanalytical methods validation and implementation, J. Chromatogr. B. 877 (2009) 2235–2243, https://doi.org/10.1016/j.jchromb.2009.06.019.
[164] International Council for Harmonization, Validation of Analytical Procedures: Text and Methodology (ICH Q2-R1), 2000 (n.d.), http://www.ich.org/. accessed February 16, 2024.

[165] A. Oliva, M. Llabrés, Uncertainty of size-exclusion chromatography method in quality control of bevacizumab batches, Separations 8 (2021) 133, https://doi.org/10.3390/separations8090133.
[166] R.J. Falconer, D. Jackson-Matthews, S.M. Mahler, Analytical strategies for assessing comparability of biosimilars, J. Chem. Technol. Biotechnol. 86 (2011) 915–922, https://doi.org/10.1002/jctb.2629.
[167] R.M. Ferretto, D.P. Leal, L.M. da Silva, D.R. Nogueira, S.L. Dalmora, Validation of a size-exclusion LC method and assessment of rhEPO in pharmaceutical formulations by liquid chromatography and biological assay, J. Liq. Chromatogr. Relat. Technol. 32 (2009) 1392–1406, https://doi.org/10.1080/10826070902900327.
[168] H.I. Kristensen, E.M. Tromborg, J.R. Nielsen, J.I. Nielsen, K.B. Johansen, P. B. Østergaard, Development and validation of a size exclusion chromatography method for determination of molecular masses and molecular mass distribution in low molecular weight heparin, Thromb. Res. 64 (1991) 131–141, https://doi.org/10.1016/0049-3848(91)90113-B.
[169] F. Jirjees, K. Soliman, Y. Wang, R. Sonawane, R. Sheshala, D. Jones, R.R. S. Thakur, A validated size exclusion chromatography method coupled with fluorescence detection for rapid quantification of bevacizumab in ophthalmic formulations, J. Pharm. Biomed. Anal. 174 (2019) 145–150, https://doi.org/10.1016/j.jpba.2019.05.038.
[170] E. Sahin, C.J. Roberts, Size-exclusion chromatography with multi-angle light scattering for elucidating protein aggregation mechanisms, in: 2012: pp. 403–423. https://doi.org/10.1007/978-1-61779-921-1_25.
[171] H.R. Doss, M. Raman, R. Knihtila, N. Chennamsetty, D. Wang, A. Shupe, N. Mussa, Streamlining the polishing step development process via physicochemical characterization of monoclonal antibody aggregates, J. Chromatogr. A. 1598 (2019) 101–112, https://doi.org/10.1016/j.chroma.2019.03.044.
[172] Y. Jing, M. Borys, S. Nayak, S. Egan, Y. Qian, S.-H. Pan, Z.J. Li, Identification of cell culture conditions to control protein aggregation of IgG fusion proteins expressed in Chinese hamster ovary cells, Process Biochem 47 (2012) 69–75, https://doi.org/10.1016/j.procbio.2011.10.009.
[173] L. Chemmalil, T. Prabhakar, J. Kuang, J. West, Z. Tan, V. Ehamparanathan, Y. Song, J. Xu, J. Ding, Z. Li, Online/at-line measurement, analysis and control of product titer and critical product quality attributes (CQAs) during process development, Biotechnol. Bioeng. 117 (2020) 3757–3765, https://doi.org/10.1002/bit.27531.
[174] Z. Chen, Y. Qian, Y. Song, X. Xu, L. Tao, N. Mussa, S. Ghose, Z.J. Li, Design of next-generation therapeutic IgG4 with improved manufacturability and bioanalytical characteristics, MAbs 12 (2020), https://doi.org/10.1080/19420862.2020.1829338.
[175] J. Rea, D. Fulchiron, L. Darer, Size-exclusion chromatography for the analysis of complex and novel biopharmaceutic products, LCGC Eur 33 (2020) 87–95.
[176] B.L. Duivelshof, A. Murisier, J. Camperi, S. Fekete, A. Beck, D. Guillarme, V. D'Atri, Therapeutic Fc-fusion proteins: current analytical strategies, J. Sep. Sci. (2020) 1–28, https://doi.org/10.1002/jssc.202000765.
[177] R. Thomas, D. Song, T. Pourmohamad, K. Kurita, S. Chin, L. Dai, A. Goyon, C. D. Medley, J.A. Gruenhagen, T. Chen, Automated online deconjugation of antibody-drug conjugate for small molecule drug profiling, J. Chromatogr. A. 1715 (2024) 464575, https://doi.org/10.1016/j.chroma.2023.464575.
[178] J. Jones, L. Pack, J.H. Hunter, J.F. Valliere-Douglass, Native size-exclusion chromatography-mass spectrometry: suitability for antibody–drug conjugate drug-to-antibody ratio quantitation across a range of chemotypes and drug-loading levels, MAbs (2020) 12, https://doi.org/10.1080/19420862.2019.1682895.
[179] E. Deslignière, H. Diemer, S. Erb, P. Coliat, X. Pivot, A. Detappe, O. Hernandez-Alba, S. Cianférani, A combination of native LC-MS approaches for the comprehensive characterization of the antibody-drug conjugate trastuzumab deruxtecan, Front. Biosci. 27 (2022) 290, https://doi.org/10.31083/j.fbl2710290.
[180] U. Brinkmann, R. Kontermann, The making of bispecific antibodies, MAbs (2017) 9, https://doi.org/10.1080/19420862.2016.1268307.
[181] B.L. Duivelshof, A. Beck, D. Guillarme, V. D'Atri, Bispecific antibody characterization by a combination of intact and site-specific/chain-specific LC/MS techniques, Talanta 236 (2022) 122836, https://doi.org/10.1016/j.talanta.2021.122836.
[182] D.A.T. Cramer, V. Franc, A.-K. Heidenreich, M. Hook, M. Adibzadeh, D. Reusch, A.J.R. Heck, M. Haberger, Characterization of high-molecular weight by-products in the production of a trivalent bispecific 2+1 heterodimeric antibody, MAbs (2023) 15, https://doi.org/10.1080/19420862.2023.2175312.
[183] A.B. Schwahn, J. Baek, S. Lin, C.A. Pohl, K. Cook, A universal eluent system for method scouting and separation of biotherapeutic proteins by ion-exchange, size-exclusion, and hydrophobic interaction chromatography, Anal. Chem. 94 (2022) 16369–16375, https://doi.org/10.1021/acs.analchem.2c03531.
[184] S. Fekete, C. Doneanu, B. Addepalli, M. Gaye, J. Nguyen, B. Alden, R. Birdsall, D. Han, G. Isaac, M. Lauber, Challenges and emerging trends in liquid chromatography-based analyses of mRNA pharmaceuticals, J. Pharm. Biomed. Anal. 224 (2023) 115174, https://doi.org/10.1016/j.jpba.2022.115174.
[185] S. Fekete, M.K. Aebischer, M. Imiołek, T. Graf, R. Ruppert, M. Lauber, V. D'Atri, D. Guillarme, Chromatographic strategies for the analytical characterization of adeno-associated virus vector-based gene therapy products, TrAC Trends Anal. Chem. 164 (2023) 117088, https://doi.org/10.1016/j.trac.2023.117088.
[186] Y.H. Chionh, C.-H. Ho, D. Pruksakorn, I.Ramesh Babu, C.S. Ng, F. Hia, M. E. McBee, D. Su, Y.L.J. Pang, C. Gu, H. Dong, E.G. Prestwich, P.-Y. Shi, P. R. Preiser, S. Alonso, P.C. Dedon, A multidimensional platform for the purification of non-coding RNA species, Nucleic Acids Res 41 (2013) e168, https://doi.org/10.1093/nar/gkt668.
[187] Y.-S. Kim, D.-H. Kim, D. An, Y. Lim, Y.-J. Seo, H.K. Kim, H.-Y. Kang, The RNA ligation method using modified splint DNAs significantly improves the efficiency of circular RNA synthesis, Animal Cells Syst. (Seoul). 27 (2023) 208–218, https://doi.org/10.1080/19768354.2023.2265165.
[188] M. Packer, D. Gyawali, R. Yerabolu, J. Schariter, P. White, A novel mechanism for the loss of mRNA activity in lipid nanoparticle delivery systems, Nat. Commun. 12 (2021) 6777, https://doi.org/10.1038/s41467-021-26926-0.
[189] Analytical procedures for mRNA vaccine quality, Draft guidelines: 2nd Ed., (2023). https://www.uspnf.com/notices/analytical-procedures-mrna-vaccines-20230428 (accessed February 16, 2024).
[190] G.J. Guimaraes, J. Kim, M.G. Bartlett, Characterization of mRNA therapeutics, Mass Spectrom. Rev. (2023), https://doi.org/10.1002/mas.21856.
[191] A. Kanavarioti, HPLC methods for purity evaluation of man-made single-stranded RNAs, Sci. Rep. 9 (2019) 1019, https://doi.org/10.1038/s41598-018-37642-z.
[192] C. Grabielle-Madelmont, S. Lesieur, M. Ollivon, Characterization of loaded liposomes by size exclusion chromatography, J. Biochem. Biophys. Methods. 56 (2003) 189–217, https://doi.org/10.1016/S0165-022X(03)00059-9.
[193] X. Jia, Y. Liu, A.M. Wagner, M. Chen, Y. Zhao, K.J. Smith, D. Some, A.M. Abend, J. Pennington, Enabling online determination of the size-dependent RNA content of lipid nanoparticle-based RNA formulations, J. Chromatogr. B. 1186 (2021) 123015, https://doi.org/10.1016/j.jchromb.2021.123015.
[194] A.L. Gimpel, G. Katsikis, S. Sha, A.J. Maloney, M.S. Hong, T.N.T. Nguyen, J. Wolfrum, S.L. Springs, A.J. Sinskey, S.R. Manalis, P.W. Barone, R.D. Braatz, Analytical methods for process and product characterization of recombinant adeno-associated virus-based gene therapies, Mol. Ther. - Methods Clin. Dev. 20 (2021) 740–754, https://doi.org/10.1016/j.omtm.2021.02.010.
[195] Y. Xie, M. Butler, Multi-attribute analysis of adeno-associated virus by size exclusion chromatography with fluorescence and triple-wavelength UV detection, Anal. Biochem. 680 (2023) 115311, https://doi.org/10.1016/j.ab.2023.115311.
[196] J.Y. Song, T. Farkas, Adeno-associated virus analysis by size exclusion chromatography within 3 min using short bio-inert columns made with 3μm particles operated at high flowrates, J. Chromatogr. A. 1718 (2024) 464684, https://doi.org/10.1016/j.chroma.2024.464684.
[197] N.L. McIntosh, G.Y. Berguig, O.A. Karim, C.L. Cortesio, R. De Angelis, A.A. Khan, D. Gold, J.A. Maga, V.S. Bhat, Comprehensive characterization and quantification of adeno associated vectors by size exclusion chromatography and multi angle light scattering, Sci. Rep. 11 (2021) 3012, https://doi.org/10.1038/s41598-021-82599-1.
[198] C. Ladd Effio, S.A. Oelmeier, J. Hubbuch, High-throughput characterization of virus-like particles by interlaced size-exclusion chromatography, Vaccine 34 (2016) 1259–1267, https://doi.org/10.1016/j.vaccine.2016.01.035.
[199] J. Vajda, D. Weber, D. Brekel, B. Hundt, E. Müller, Size distribution analysis of influenza virus particles using size exclusion chromatography, J. Chromatogr. A. 1465 (2016) 117–125, https://doi.org/10.1016/j.chroma.2016.08.056.
[200] K. Lundstrom, Viral vectors in gene therapy: where do we stand in 2023? Viruses 15 (2023) 698, https://doi.org/10.3390/v15030698.
[201] H. Small, F.L. Saunders, J. Solc, Hydrodynamic chromatography A new approach to particle size analysis, Adv. Colloid Interface Sci. 6 (1976) 237–266, https://doi.org/10.1016/0001-8686(76)85004-X.
[202] A.M. Striegel, Hydrodynamic chromatography: packed columns, multiple detectors, and microcapillaries, Anal. Bioanal. Chem. 402 (2012) 77–81, https://doi.org/10.1007/s00216-011-5334-3.
[203] I.K. Ventouri, W. Chang, F. Meier, R. Drexel, G.W. Somsen, P.J. Schoenmakers, B. de Spiegeleer, R. Haselberg, A. Astefanei, Characterizing non-covalent protein complexes using asymmetrical flow field-flow fractionation on-line coupled to native mass spectrometry, Anal. Chem 95 (2023) 7487–7494, https://doi.org/10.1021/acs.analchem.2c05049.
[204] F. Gritti, Resolution limits of size exclusion chromatography columns identified from flow reversal and overcome by recycling liquid chromatography to improve the characterization of manufactured monoclonal antibodies, J. Chromatogr. A. 1705 (2023) 464219, https://doi.org/10.1016/j.chroma.2023.464219.
[205] A. Ehkirch, O. Hernandez-Alba, O. Colas, A. Beck, D. Guillarme, S. Cianférani, Hyphenation of size exclusion chromatography to native ion mobility mass spectrometry for the analytical characterization of therapeutic antibodies and related products, J. Chromatogr. B Anal. Technol. Biomed. Life Sci. 1086 (2018) 176–183, https://doi.org/10.1016/j.jchromb.2018.04.010.